Lin...
G...11

P-104

T · H · E
OHIO STATE UNIVERSITY

DESIGN OF BLENDED ROLLED EDGES FOR COMPACT RANGE MAIN REFLECTORS

K.P. Ericksen
I.J. Gupta
W.D. Burnside

The Ohio State University

ElectroScience Laboratory

Department of Electrical Engineering
Columbus, Ohio   43212

NOTICES

When Government drawings, specifications, or other data are used for any purpose other than in connection with a definitely related Government procurement operation, the United States Government thereby incurs no responsibility nor any obligation whatsoever, and the fact that the Government may have formulated, furnished, or in any way supplied the said drawings, specifications, or other data, is not to be regarded by implication or otherwise as in any manner licensing the holder or any other person or corporation, or conveying any rights or permission to manufacture, use, or sell any patented invention that may in any way be related thereto.

REPORT DOCUMENTATION PAGE	50272-101				
	1. REPORT NO.	2.		3. Recipient's Accession No	
4. Title and Subtitle				5. Report Date	August 1988
DESIGN OF BLENDED ROLLED EDGES FOR COMPACT RANGE MAIN REFLECTORS				6.	
7. Author(s) K.P. Ericksen, I.J. Gupta and W.D. Burnside				8. Performing Organization Rept. No 716148-33	
9. Performing Organization Name and Address				10. Project/Task/Work Unit No	
THE OHIO STATE UNIVERSITY ELECTROSCIENCE LABORATORY 1320 Kinnear Road Columbus, Ohio 43212				11. Contract(C) or Grant(G) No (C) (G) NSG-1613	
12. Sponsoring Organization Name and Address				13. Type of Report & Period Covered	
NATIONAL AERONAUTICS AND SPACE ADMINISTRATION Langley Research Center Hampton, VA 23665				Technical	
				14.	

15. Supplementary Notes

16. Abstract (Limit: 200 words)

A procedure to design blended rolled edge terminations for arbitrary rim shape compact range main reflectors is presented. The reflector may be center-fed or offset-fed. The design procedure leads to a reflector which has a continuous and smooth surface. This procedure also ensures small diffracted fields from the junction between the paraboloid and the blended rolled edge while satisfying certain constraints regarding the maximum height of the reflector and minimum operating frequency of the system. The prescribed procedure is used to design several reflectors and the performance of these reflectors is presented.

17. Document Analysis a. Descriptors

b. Identifiers/Open-Ended Terms

c. COSATI Field/Group

18. Availability Statement	19. Security Class (This Report) Unclassified	21. No of Pages 93
	20. Security Class (This Page) Unclassified	22. Price

(See ANSI-Z39.18)   See Instructions on Reverse   OPTIONAL FORM 272 (4-77) (Formerly NTIS-35) Department of Commerce

i

ACKNOWLEDGEMENTS

iii

TABLE OF CONTENTS

REFERENCES

LIST OF FIGURES

LIST OF TABLES

CHAPTER I

INTRODUCTION

For accurate radar cross section (RCS) measurements, one should illuminate the target with a plane wave. One way to achieve a plane wave is to use a compact antenna range [1]. In a compact range, a paraboloid is normally used as the main reflector with a point source at the focus. The paraboloid converts the spherical wavefront of the point source to a planar wavefront. However, because a finite size paraboloid is used in a compact range, there are diffracted fields from the rim of the paraboloid. These diffracted fields disrupt the planar wavefront and cause erroneous measurements. In order to reduce the diffracted fields, various edge termination methods have been investigated. These methods include: the use of absorber material [2], serrated edges [2], shaped reflectors [3], simple rolled edge [4], and blended rolled edges [5,6]. Among these methods, rolled edge terminations seem to provide the best performance. For a rolled edge termination, an elliptical or some similar surface is added to the paraboloid along its rim such that the surface is smooth and continuous. Thus the diffracted field level from the rim of the paraboloid (junction contour) is reduced. Also, since the specular reflection from the rolled edge is away from the target area, the planar wavefront is maintained. Recently, the concept of blended rolled edges has been introduced. In a blended rolled edge, the elliptical rolled edge is blended with an extension of the parabola using a blending function. The use of a blending function smooths the junction

1

even further in that the radius of curvature and a certain number of its derivatives are continuous across the junction [5]. However, the resulting reflector may be too large to be practical. Also, the minimum radius of curvature of the reflector surface in the lit region may be less than desired. Thus, the choice of the blending function and blending parameters are quite important in the design of compact range reflectors with blended rolled edges.

Gupta *et al.* [7] have developed a method to design blended rolled edges for two-dimensional and circular symmetric reflectors. That method leads to a rolled edge which minimizes the edge diffracted fields while satisfying certain constraints regarding reflector size and minimum operating frequency. The rolled edge is defined in the plane which contains the focal point of the paraboloid for any point on the rim of the paraboloid. In this study, the design method is extended to three-dimensional paraboloids with arbitrary junction contours. The reflectors may be center-fed or offset-fed. Using this design procedure, one obtains a reflector with a smooth and continuous surface that also satisfies the constraints regarding reflector height and minimum operating frequency.

In the design procedure developed in this report, the rolled edge plane for each point on the junction contour is defined. This rolled edge plane is chosen so that the rolled edge surface is unique and continuous. The continuity of the specularly reflected field is also guaranteed. However, this rolled edge plane may not contain the focal point of the paraboloid. Therefore, the concept of an "equivalent parabola" is introduced. The equivalent parabola traces the contour of the paraboloid in the rolled edge plane and has its focal point in the rolled edge plane. Using the equivalent parabola, the blending parameters are found for each point on the junction contour. This is required since the equivalent parabola may be different for various points on the junction so that the blending parameters will be

2

different along the junction contour. The design procedure presented here is used to design blended rolled edges for various compact range reflectors. Performance of some of these reflectors is also studied.

The rest of this report is organized as follows. In Chapter II, the concept of the blended rolled edge as applied to two-dimensional reflectors is presented. First, the method of adding a simple rolled edge is developed. Then the procedure to design the blended rolled edge is given. Some design examples are also given. In Chapter III, the design procedure given in Chapter II is extended to three-dimensional paraboloids with arbitrary junction contours. First, the rolled edge plane is defined. Then the concept of an equivalent parabola is introduced. It is shown that the equivalent parabola is different for different points on the junction contour. Next, a complete design procedure is outlined. Finally, some reflectors are designed using the procedure. In Chapter IV, the performance of some of the reflectors designed in Chapter III is studied. It is shown that for the best performance, one should choose the reflector with a fully optimized, blended rolled edge. Chapter V includes a summary and some general conclusions of this work.

CHAPTER II

TWO-DIMENSIONAL EDGE TREATMENT OF THE MAIN REFLECTOR

2.1 Introduction

In this chapter a procedure to design blended rolled edges for two-dimensional, compact range, main reflectors is developed. A two-dimensional reflector system is equivalent to an infinitely long parabolic cylinder with an infinitely long, line focus. For this system there is no variation along the axis of the cylinder. Therefore all analyses and examples in this chapter are done in a plane perpendicular to the axis of the cylinder. A simple rolled edge is first developed which will provide a termination to the paraboloid that has slope continuity. Next, "blending functions" are introduced to further smooth the junction by gradually transforming the parabola into the simple rolled edge. Finally a procedure is developed to design blended rolled edges that satisfy the design constraints of maximum reflector height and minimum operating frequency.

2.2 Adding a simple rolled edge termination

Let the x-axis be the axis of the infinite cylinder. The plane perpendicular to this axis is the yz-plane which is used to define the two-dimensional parabola. For a parabola with a focal length, f_c, the defining equation in the yz-plane is given

by

$$z = \frac{y^2}{4f_c}.$$ (2.1)

These axes are shown in Figure 1.

Let a finite section of this parabola, $y = y_{bot}$ to $y = y_{top}$, be used as the main reflector in the compact range as shown in Figure 1. This results in a reflected field which is discontinuous at the edges of the parabola. Thus there will be strong diffracted fields from the edges of the parabola. To decrease the magnitude of the diffracted fields from the top ($y = y_{top}$) and bottom ($y = y_{bot}$) edges of the parabola, let elliptic rolled edges [4] be added to the top and bottom edges (junctions). The edges where the terminations are added are defined by the point $P_j(y_j, z_j)$, where $y_j = y_{top}$ indicates the top edge (junction), and $y_j = y_{bot}$ indicates the bottom edge (junction). From the definition of the parabola given in Equation (2.1), the z coordinate of the junction is

$$z_j = \frac{y_j^2}{4f_c}.$$ (2.2)

The simple rolled edge termination added to the parabola is elliptic in cross section as shown in Figure 2. The ellipse is added such that the surface tangent is continuous at the junction. The addition of the ellipse must also satisfy the maximum reflector height and minimum operating frequency requirements. Note that the elliptic surface curves away from the focus of the parabola so that the reflected field from the rolled edge is out of the target zone. A method to add elliptical rolled edges is given below.

2.2.1 Ellipse coordinate system

As mentioned above, the rolled edge should be added to the parabola such that the slopes of the two surfaces (parabola and ellipse) are continuous at the
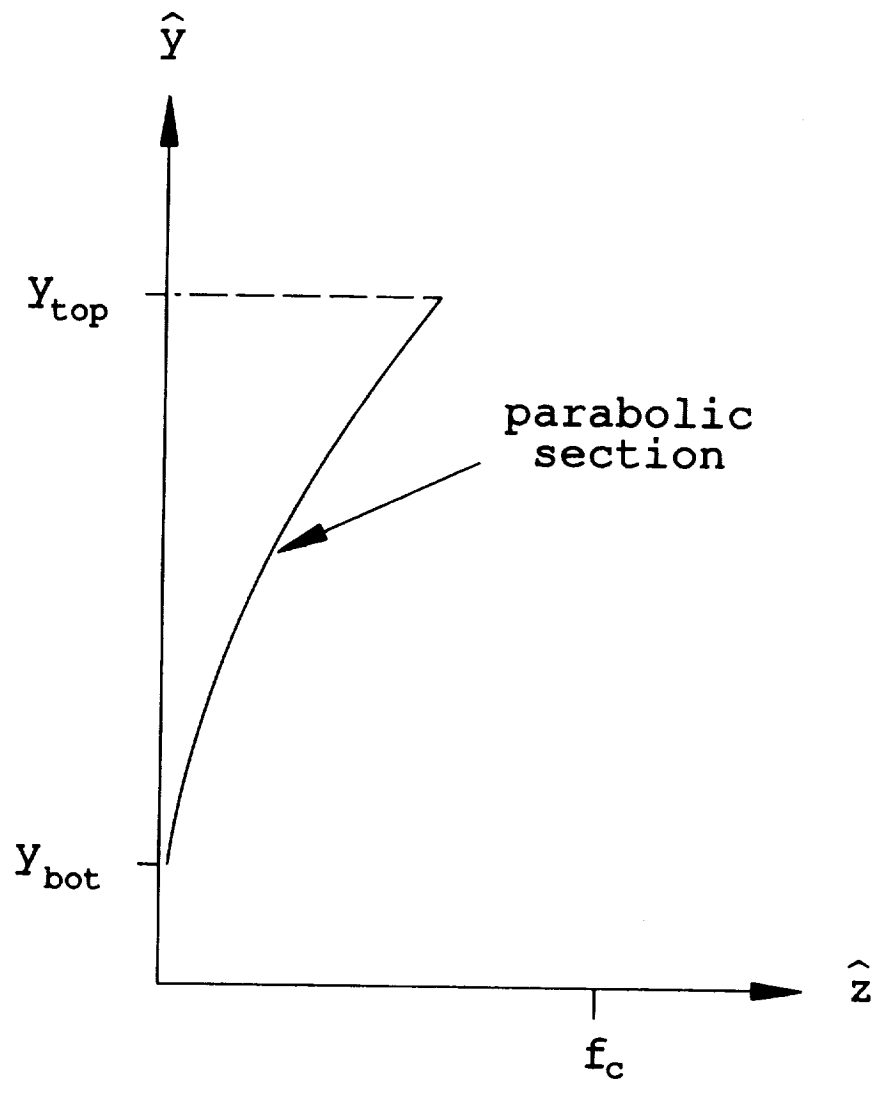
Figure 1: Section of parabola used as a main reflector in a compact range.

junction. To do so, it is convenient to set up a local coordinate system centered at the junction between the ellipse and the parabola. This local coordinate system is referred to as (x_e, y_e) and is shown in Figure 2 . To make the slopes of the ellipse and parabola continuous, it is necessary that the tangent to both surfaces at the junction be parallel. By defining the y_e-direction as [5]

$$\hat{y}_e = -\hat{n}_j \tag{2.3}$$

where $\hat{n}_j$ is normal to the parabola at the junction, the two surface tangents will be aligned in the x_e-direction. Thus, the elliptical rolled edge should be added such that x_e and y_e are the two axes of the ellipse. The ellipse coordinate axes are then given by

$$\hat{x}_e = x_{p2}\hat{y} + x_{p3}\hat{z} \text{ , and} \tag{2.4}$$

$$\hat{y}_e = y_{p2}\hat{y} + y_{p3}\hat{z} \text{ .} \tag{2.5}$$

Note that the coordinate values are given by

$$y_{p2} = \frac{y_j}{\sqrt{y_j^2 + 4f_c^2}} \tag{2.6}$$

$$y_{p3} = \frac{-2f_c}{\sqrt{y_j^2 + 4f_c^2}} \tag{2.7}$$

$$x_{p2}(y_{top,bot}) = \mp y_{p3} \text{ , and} \tag{2.8}$$

$$x_{p3}(y_{top,bot}) = \pm y_{p2} \text{ .} \tag{2.9}$$

Using the coordinate values given in Equations (2.6)– (2.9), the coordinate transformation between the (x_e, y_e) system and the (y, z) system is given by

$$\begin{pmatrix} y(\gamma) \\ z(\gamma) \end{pmatrix} = \begin{pmatrix} x_{p2} & y_{p2} \\ x_{p3} & y_{p3} \end{pmatrix} \begin{pmatrix} x_e(\gamma) \\ y_e(\gamma) \end{pmatrix} + \begin{pmatrix} y_j \\ z_j \end{pmatrix} \tag{2.10}$$

7
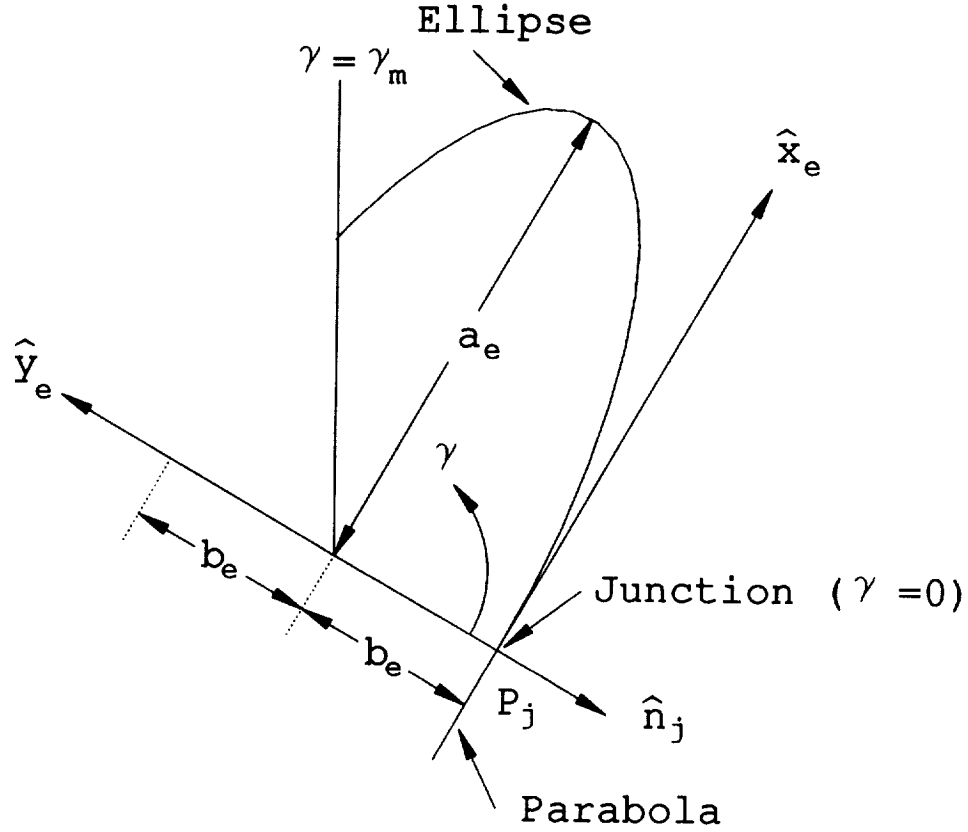
Figure 2: The addition of an elliptic termination to the parabola with slope continuity at the junction.

with the parametric angle, γ, of the rolled surface defined in the region specified by

$$0 \leq \gamma \leq \gamma_m .$$ (2.11)

In this case, γ_m is the maximum value of γ. The parameterization of the simple rolled edge as a function of γ will next be formulated.

2.2.2 Rolled edge parameterization

The parameterized equation that defines the ellipse in the (x_e, y_e) system is given as

$$\mathbf{r_e}(\gamma) = x_e(\gamma)\,\hat{\mathbf{x}}_e + y_e(\gamma)\,\hat{\mathbf{y}}_e .$$ (2.12)
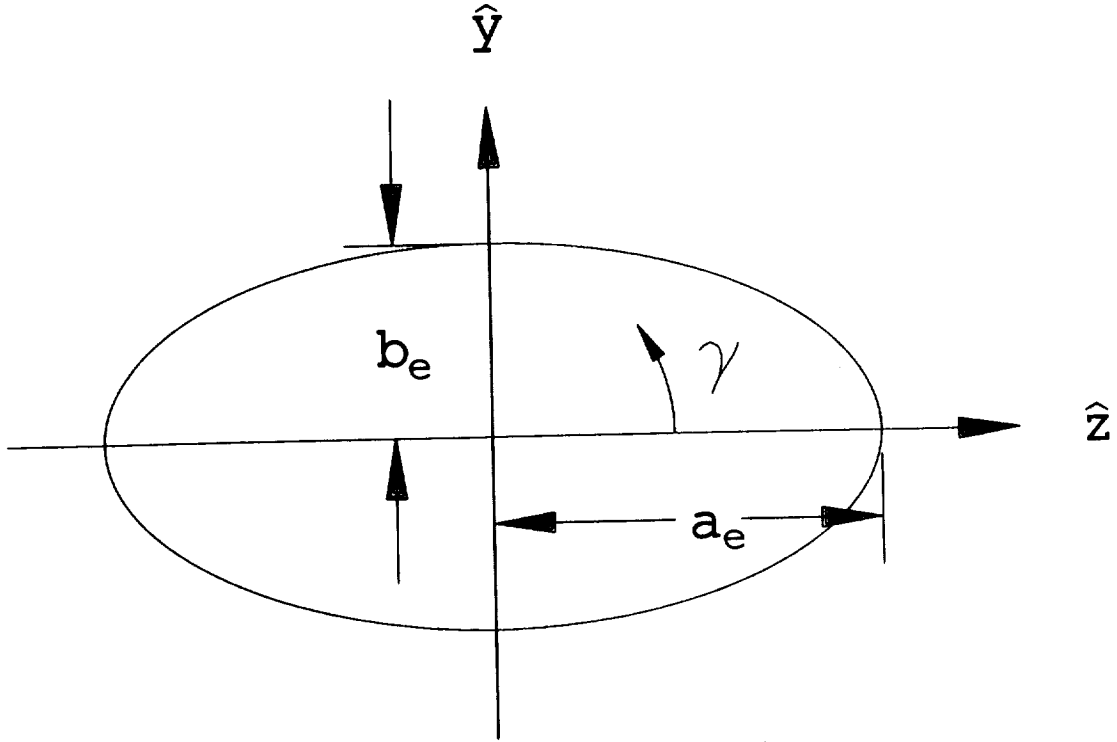
Figure 3: Central ellipse used to parameterize the simple rolled edge.

In order to parameterize the ellipse, first consider an ellipse with its center at the origin of the (y, z) coordinate system as shown in Figure 3. The parameterization of this ellipse as a function of the parametric angle, γ, is

$$\mathbf{r}(\gamma) = b_e \sin\gamma\,\hat{\mathbf{y}} + a_e \cos\gamma\,\hat{\mathbf{z}} \tag{2.13}$$

where a_e is the semi-major axis, and b_e is the semi-minor axis. Therefore, the parameterization in the (x_e, y_e) system for the offset ellipse shown in Figure 2 is given by

$$x_e(\gamma) = a_e \sin\gamma \ , \ \text{and} \tag{2.14}$$

$$y_e(\gamma) = b_e(1 - \cos\gamma)\,. \tag{2.15}$$

9

Substituting Equations (2.14) and (2.15) into Equation (2.12) gives

$$\mathbf{r_e}(\gamma) = a_e \sin\gamma\, \hat{\mathbf{x}}_e + b_e(1 - \cos\gamma)\hat{\mathbf{y}}_e \ .\qquad (2.16)$$

The ellipse can also be described in the (y, z) system of Figure 1 as

$$\mathbf{r_{ellipse}}(\gamma) = y_{ellipse}(\gamma)\hat{\mathbf{y}} + z_{ellipse}(\gamma)\hat{\mathbf{z}} \ .\qquad (2.17)$$

Substituting Equations (2.14) and (2.15) into Equation (2.10) gives

$$y_{ellipse}(\gamma) = (a_e \sin\gamma)x_{p2} + b_e(1 - \cos\gamma)y_{p2} + y_j \ , \text{ and}\qquad (2.18)$$

$$z_{ellipse}(\gamma) = (a_e \sin\gamma)x_{p3} + b_e(1 - \cos\gamma)y_{p3} + z_j \ .\qquad (2.19)$$

The total surface is given in two parts. For $y_{bot} < y < y_{top}$, the surface is parabolic as defined in Equation (2.1). For $y > y_{top}$ or $y < y_{bot}$, the surface is given by Equations (2.18) and (2.19) as a function of the parametric angle, γ . A procedure to design the simple rolled edges developed in this section is given next.

2.3 Simple rolled edge design

The objective of designing rolled edges is to make the surface of the reflector as smooth as possible. As shown in the previous section, by proper orientation, the slope of the ellipse used as a simple rolled edge has been made equal to the slope of the parabola at the junction. However, there is still a discontinuity in the radius of curvature across the junction. This can be seen from the expressions for the radius of curvature for the two surfaces at the junction. The radius of curvature of the parabola at the junction is given by [5]

$$R_c(y_j) = \left| 2f_c \left[1 + \left(\frac{y_j}{2f_c} \right)^2 \right]^{\frac{3}{2}} \right|\qquad (2.20)$$

10

and the radius of curvature of the ellipse at the junction is

$$R_c(y_j) = \left| \frac{a_e^2}{b_e} \right| . \tag{2.21}$$

The absolute value is used in Equations (2.20) and (2.21) since the radii of curvature for the ellipse and parabola are of different sign. In order to make the two radii of curvature equal, either a_e must be made very large or b_e must be made very small. For a large a_e, the reflector may to be too large to fit in a room. For a small b_e, the shadow boundaries of the reflector look like knife edges and diffract like wedges at low frequencies. Therefore, a_e and b_e are determined from a set of specified design constraints. The design constraints are the maximum allowable height (y_{max}) and minimum operating frequency. Let λ_{max} be the wavelength at the minimum operating frequency. From past observations [8], the minimum radius of curvature in the lit region of the reflector should be $\lambda_{max}/4$.

There is only one set of values for a_e and b_e which will satisfy both design constraints. In order to satisfy the height constraint, the maximum value of $y_{ellipse}$ from Equation (2.18) must be y_{max}. To ensure this condition, the derivative of Equation (2.18) with respect to γ is set equal to zero. This gives the angle of maximum height as

$$\gamma_{max} = \arctan \left(-\frac{a_e x_{p2}}{b_e y_{p2}} \right) . \tag{2.22}$$

Substituting γ_{max} and y_{max} into Equation (2.18) gives

$$y_{max} = (a_e \sin \gamma_{max}) x_{p2} + b_e (1 - \cos \gamma_{max}) y_{p2} + y_j . \tag{2.23}$$

The minimum operating frequency constraint gives the equation [5]

$$\frac{b_e^2}{a_e} = \frac{\lambda_{max}}{4} . \tag{2.24}$$

11

Table 1: Surface characteristics for elliptic rolled edge example

f_c	$7.25'$
y_{max}	$15'$
y_{top}	$11.5'$
y_{bot}	$5.5'$
a_e	$3.917'$
b_e	$0.6938'$

Therefore, solving Equations (2.23) and (2.24), the parameters a_e and b_e can be found such that the simple rolled edge will meet the design constraints. In the next section, a simple rolled edge is designed using the given procedure.

2.3.1 Example

As an example, simple rolled edges are designed for a parabola with a focal length of $7.25'$, a top junction of $11.5'$, a bottom junction of $5.5'$, and a maximum reflector height of $15'$. Thus the height of the rolled edge is $3.5'$. For a minimum operating frequency of $2\ GHz$, Equations (2.23) and (2.24) are used to find a_e and b_e. The complete surface characteristics for this reflector are given in Table 1. Figure 4 shows the surface with elliptic rolled edges generated using the characteristics given in Table 1.

To study the performance of the reflector, the scattered fields from the reflector shown in Figure 4 were computed when a Gregorian subreflector is used for illumination. In calculating the total scattered field, it is assumed that there is no direct illumination from the feed or diffraction from the subreflector. The field pattern is calculated assuming that the main reflector is illuminated only by the geometrical optics (GO) field reflected from the subreflector [5]. The subreflec-
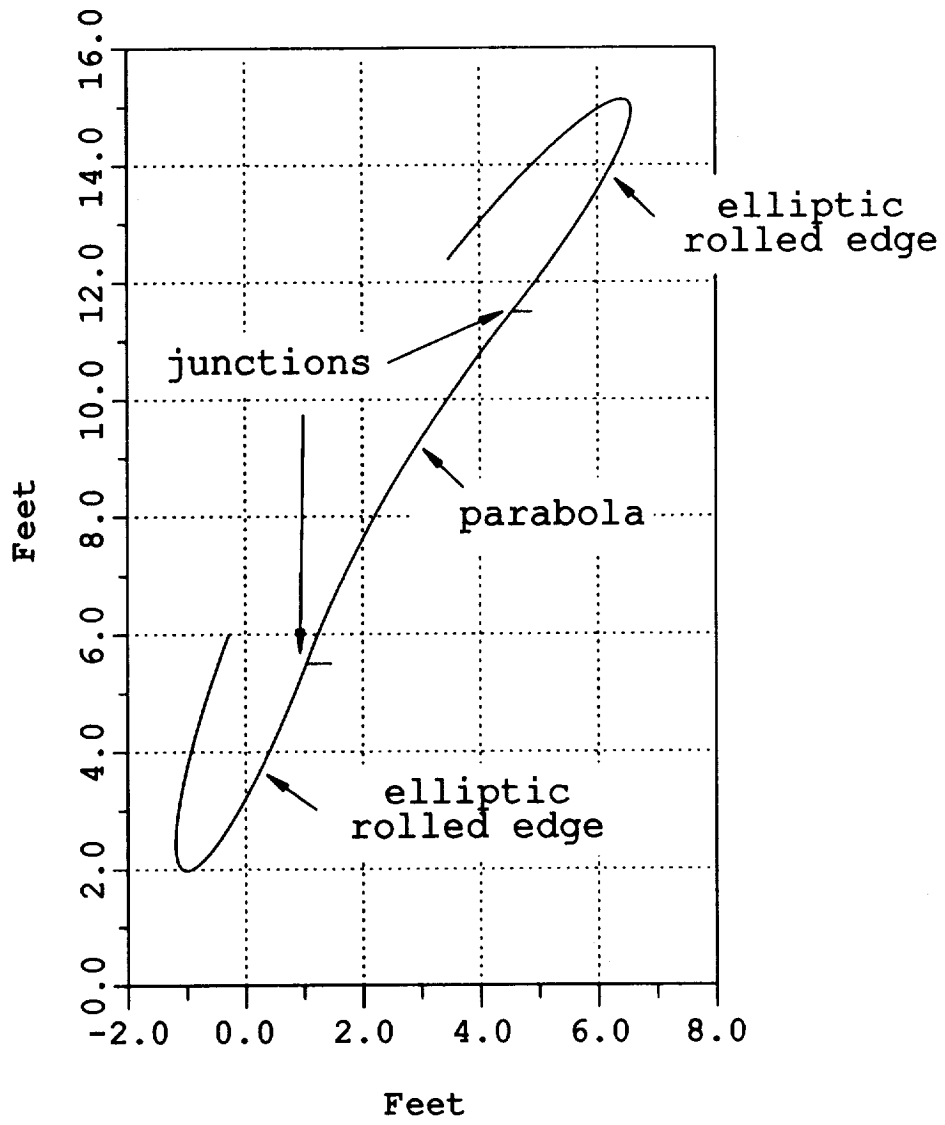
Figure 4: Example of a two-dimensional parabolic reflector with elliptic rolled edges.

13

Table 2: System characteristics for the dual reflector configuration

β	$5.5°$
α	$20°$
a_{sr}	$5.25'$
b_{sr}	$4.308'$

tor eliminates the feed blockage problem and also minimizes the amplitude taper and cross-polarization errors in the reflected plane wave [9,10]. This dual reflector system is shown in Figure 5.

In order to find the scattered and diffracted fields from the reflector with simple rolled edges, there are certain system characteristics which must be determined. These characteristics, as shown in Figure 5 are: tilt (β) of the subreflector main axis with respect to axis of symmetry of the parabola, tilt of the axis of symmetry (z_f axis) of the primary feed antenna relative to the main axis of the subreflector (α), subreflector semi-major axis length (a_{sr}) and semi-minor axis length (b_{sr}). The specific values used for this example are given in Table 2 [5]. Since this is a two-dimensional problem, the primary feed antenna is an infinitely long y-polarized Huygen's line source with unit amplitude.

Physical optics (PO) can be used to calculate the scattered field from the main reflector. However, conventional physical optics will give false scattering from the incident shadow boundary. This is due to the fact that conventional PO assumes the wrong induced surface currents at the shadow boundary. The surface currents are assumed to be zero in the shadow regions of the structure. This sudden discontinuity of the induced surface currents across the shadow boundary creates false scattering at the incident shadow boundaries. Therefore, the method used

14
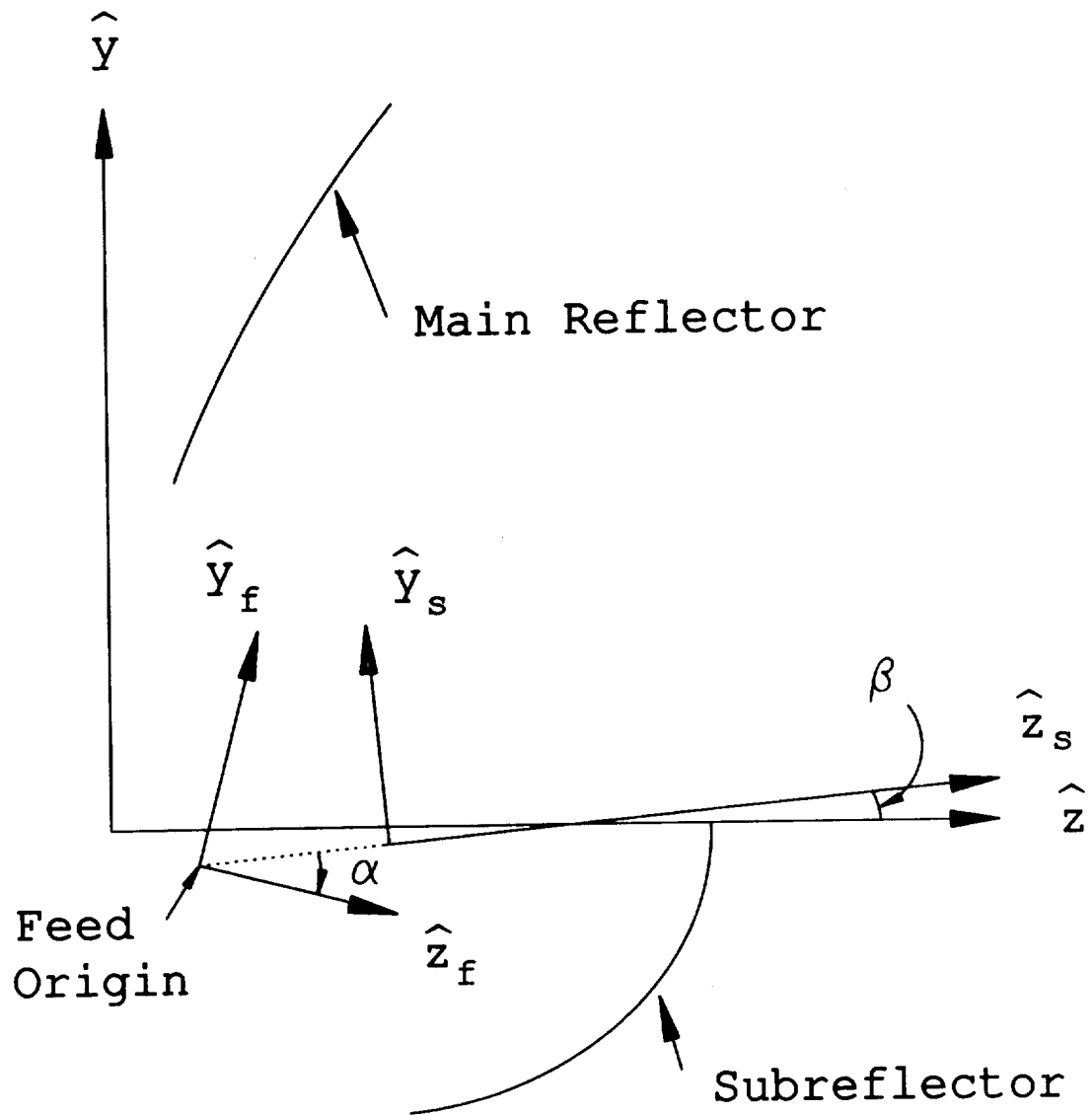
Figure 5: Dual reflector compact range configurations.

for the field calculations is a corrected PO solution [11]. The correction is made by subtracting the shadow boundary (end point) contributions from the conventional PO results.

The total scattered field for this reflector is shown in Figure 6 and the total diffracted fields due to the junction discontinuities are shown in Figure 7. The diffracted fields are found by subtracting the GO field from the corrected PO results. Both fields are plotted relative to the GO field in the target zone.

Note that the diffracted fields in the entire target zone ($y = 5.5'$ to $11.5'$), are at least $12\,dB$ below the GO fields. As expected, the diffracted fields are the strongest near the edges ($y = 5.5'$ and $11.5'$). Without any edge termination, the diffracted fields will be within $6\,dB$ of the GO fields. Thus, the rolled edge has reduced the diffracted fields in the target zone. However, the ripple in the total scattered fields in the target zone is still quite large. For accurate measurements, the ripple should be less than $0.2\,dB$ [12]. For a $0.2\,dB$ ripple requirement, the diffracted fields should be at least $32\,dB$ below the GO fields. Thus, the diffracted fields should be futher reduced. One way to further reduce the diffracted fields is to smoothly blend the rolled edge from a parabola to an ellipse [6]. This leads to a blended rolled edge. In the next section, a procedure is developed using blending functions to form a blended rolled edge.

2.4   Blended rolled edge terminations

To further reduce the unwanted diffracted fields in the target zone, the radius of curvature of the reflector should be made continuous across the junction. A blended rolled edge [5] can be used to meet this goal. A blended rolled edge is generated by blending the simple rolled edge with a part of the paraboloid using a blending function. The use of a blending function ensures that the radius of
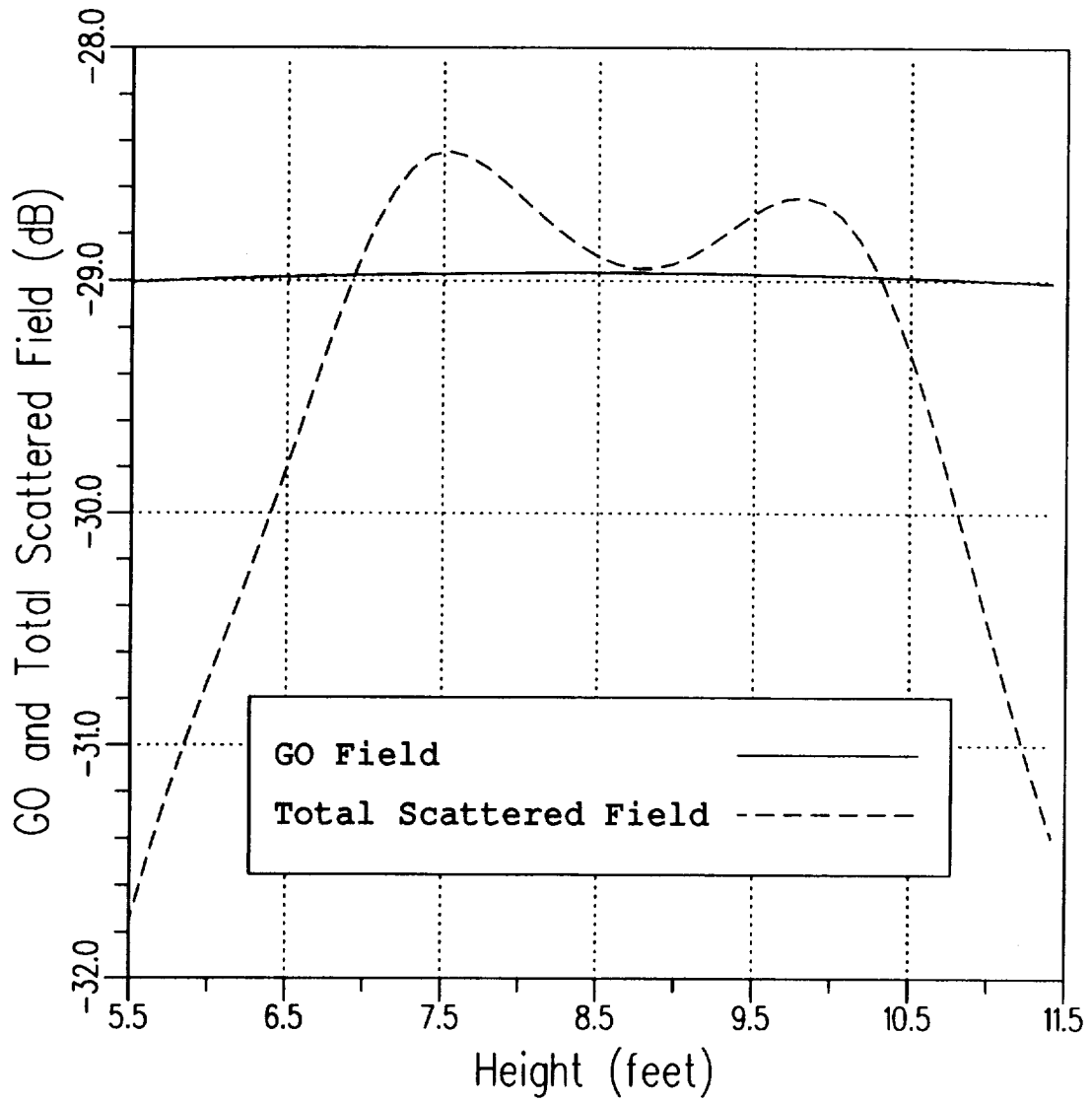
Figure 6: Total scattered field 20' from a reflector with a simple rolled edge.
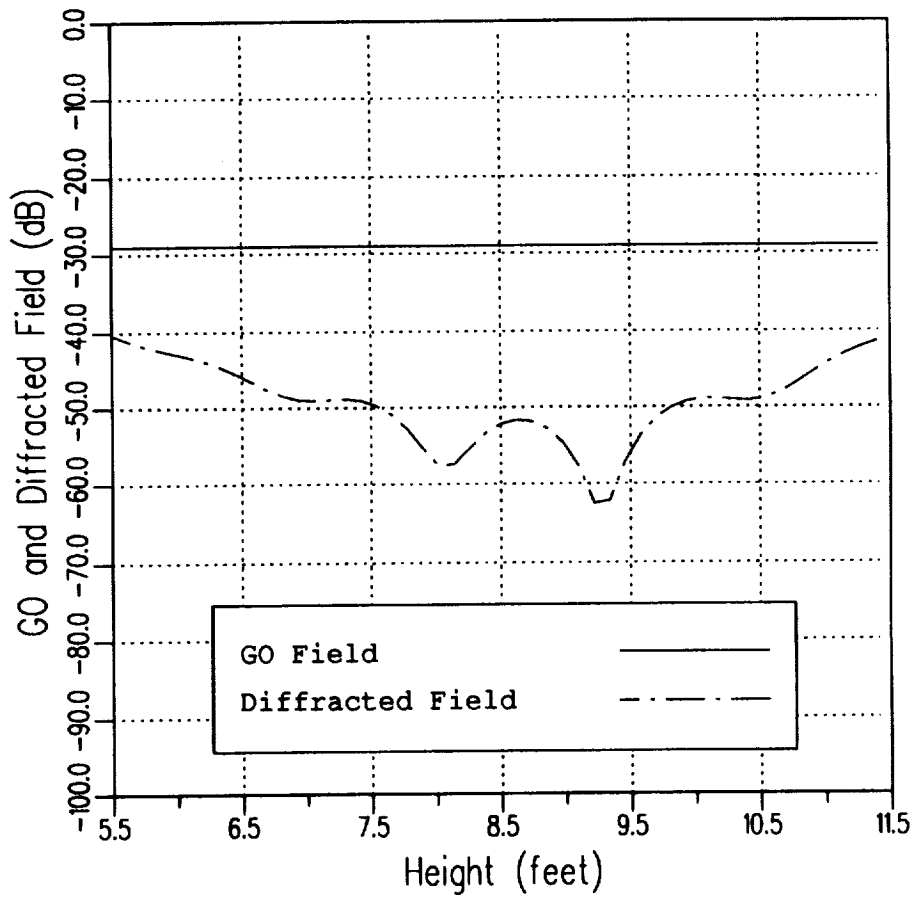
Figure 7: Diffracted field 20' from a reflector with a simple rolled edge.

18

curvature of the surface is continuous across the junction [5]. Also, depending on the type of blending function used, the first few derivatives of the radius of curvature can be made continuous across the junction.

As with the simple rolled edge, let the blending function be specified by the parametric angle, γ. Within the range of the parametric angle, $0 \leq \gamma \leq \gamma_m$, it is desired that the blending function, $b(\gamma)$, vary from 0 to 1. At $\gamma = 0$, $b(0) = 0$ and the surface is parabolic. For $\gamma = \gamma_m$, then $b(\gamma_m) = 1$, and the surface is elliptic. In this way the blended surface can be described by the following equation [8,6]:

$$f_{blend}(\gamma) = f_{parabola}(\gamma)[1 - b(\gamma)] + f_{ellipse}(\gamma) b(\gamma) . \qquad (2.25)$$

The $f_{parabola}$ term is the extension of the parabolic surface beyond the junction as shown in Figure 8. Note that the blended rolled edge is attached to the parabola at the point, P_j, exactly as the ellipse is added in Section 2.2. The local coordinate system used to add the blended rolled edge is the same as described in Equations (2.3) - (2.9).

One can choose a blending function such that its value and first $n - 1$ derivatives are zero at the junction where $n = 1, 2, 3 \ldots$. Such a function will be called an n-th order blending function. Thus, for an n-th order blending function,

$$b^{(n)}(0) \neq 0 , \text{ and} \qquad (2.26)$$

$$b^{(m)}(0) = 0 , m = 1, 2, \ldots, n - 1 . \qquad (2.27)$$

For an n-th order blending function it can be shown [5] that the radius of curvature and its first $n - 1$ derivatives are equal to zero at the junction. Since the $n - 1$ derivatives of the blending function are zero at the junction, this ensures that the $n - 1$ derivatives of the radius of curvature are continuous across the junction [5]. Therefore, the junction between the parabola and a blended rolled edge is smoother than the junction obtained from adding a simple rolled edge.

19
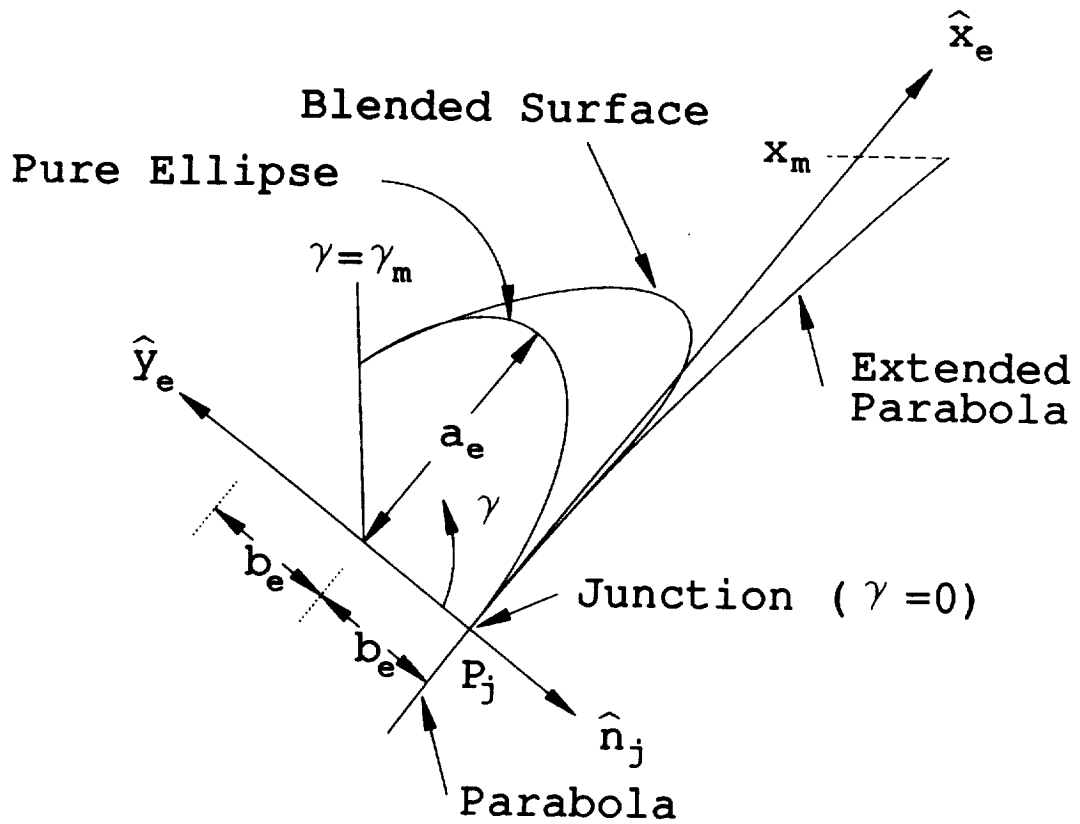
Figure 8: Blending the rolled edge termination.

A few blending functions and their order are presented below:

1. First order ($b(0) = 0$, $b'(0) \neq 0$)

   Linear blending:

   $$b(\gamma) = \frac{\gamma}{\gamma_m} \qquad (2.28)$$

2. Second order ($b(0) = 0$, $b'(0) = 0$, $b''(0) \neq 0$)

   Square blending:

   $$b(\gamma) = \left(\frac{\gamma}{\gamma_m}\right)^2 \qquad (2.29)$$

   Cosine blending:

   $$b(\gamma) = \frac{1}{2}\left(1 - \cos\frac{\pi\gamma}{\gamma_m}\right) \qquad (2.30)$$

3. Fourth order ($b(0) = 0$, $b'(0) = 0$, $b''(0) = 0$, $b^{iv}(0) \neq 0$)

   Cosine squared blending:

   $$b(\gamma) = \frac{1}{4}\left(1 - \cos\frac{\pi\gamma}{\gamma_m}\right)^2 \qquad (2.31)$$

The complete blended surface can now be defined. For a two-dimensional surface, Equation (2.25) will have y and z coordinates. These are defined as

$$y_{blend}(\gamma) = y_{parabola}(\gamma)[1 - b(\gamma)] + y_{ellipse}(\gamma)b(\gamma) \text{ , and} \qquad (2.32)$$

$$z_{blend}(\gamma) = z_{parabola}(\gamma)[1 - b(\gamma)] + z_{ellipse}(\gamma)b(\gamma) . \qquad (2.33)$$

The extended parabola that is to be blended to the rolled edge will have a maximum value defined as, x_m, as measured along the x_e-axis. The $y_{parabola}$ term from Equation (2.32) can then be described as a linear displacement along this x_e-axis as

$$y_{parabola}(\gamma) = \gamma\left(\frac{x_m}{\gamma_m}\right)x_{p2} + y_j . \qquad (2.34)$$

21

The $z_{parabola}$ term found from Equation (2.1) is

$$z_{parabola}(\gamma) = \frac{[y_{parabola}(\gamma)]^2}{4f_c} .$$ (2.35)

When $\gamma = \gamma_m$, Equation (2.34) gives the maximum value of the extended parabola as $x_m x_{p2} + y_j$. This is the section of the parabola that is blended with the ellipse to give the complete blended rolled edge termination.

By substituting Equations (2.18) and (2.34) into Equation (2.32), and also substituting Equations (2.19) and (2.35) into Equation (2.33), the general two-dimensional blended rolled surface can be expressed in the (y, z) system as

$$
\begin{aligned}
y_{blend}(\gamma) = {} & \left[\gamma \left(\frac{x_m}{\gamma_m} \right) x_{p2} + y_j \right] [1 - b(\gamma)] \\
& + [(a_e \sin \gamma) x_{p2} + b_e(1 - \cos \gamma) y_{p2} + y_j] b(\gamma)
\end{aligned}
$$ (2.36)

and

$$
\begin{aligned}
z_{blend}(\gamma) = {} & \left(\frac{[\gamma(x_m/\gamma_m) x_{p2} + y_j]^2}{4f_c} \right) [1 - b(\gamma)] \\
& + [(a_e \sin \gamma) x_{p3} + b_e(1 - \cos \gamma) y_{p3} + z_j] b(\gamma) .
\end{aligned}
$$ (2.37)

The total surface is again given in two parts. For $y_{bot} < y < y_{top}$, the surface is parabolic as given by Equation (2.1). For $y > y_{top}$ or $y < y_{bot}$, the new blended surface is described by Equations (2.36) and (2.37) as a function of the parametric angle, γ.

The terms a_e, b_e, x_m, and γ_m used in Equations (2.36) and (2.37) are the four blending parameters that are used to define the blended rolled edge termination. Depending on the maximum available reflector height and target zone size, a blending function can be chosen which will minimize the diffracted fields due to the junction discontinuity between the parabola and the blended rolled edge termination [5]. Therefore, the next step in the design procedure is to find the blending

22

parameters so that the design constraints applied to the reflector are satisfied. A procedure to find these parameters is given next.

2.5 Blended rolled edge design

In Sections 2.2 and 2.4, a procedure has been developed to add a blended rolled edge to a compact range, main reflector. The design parameters for the main reflector are focal length (f_c), junction height (y_j), total available height (y_{max}), minimum operating frequency (f_{min}), and choice of a blending function $(b(\gamma))$. The difference between the maximum height and the top of the parabola specifies the amount of rolled edge to be added. This is defined as

$$r_e = y_{max} - y_{top} \; . \tag{2.38}$$

In order to design a blended rolled edge for a main reflector, the blending parameters a_e, b_e, x_m, and γ_m must be determined. It is desired to find an optimum set of blending parameters which also satisfy the constraints regarding the available height and the minimum operating frequency. The optimum set of blending parameters is defined as the one which minimizes the surface discontinuity at the junction.

For a specific blending function used to add the rolled edge, the first non-continuous derivative of the radius of curvature is the discontinuity that should be minimized. For an n-th order blending function as defined in Section 2.4, the discontinuity at the junction is found from the expressions for the derivatives of the radius of curvature on both sides of the junction. Since for a n-th order blending function the first $n - 1$ derivatives are continuous across the junction, then

$$\left(\frac{d^m R_c}{dy^m}\right)^{blend} = \left(\frac{d^m R_c}{dy^m}\right)^{parabola} , m = 1, 2, \ldots, n - 1 \; . \tag{2.39}$$

Table 3: $\alpha_n \, b^n(0)$ for various blending functions

Order	Type	$\alpha_n \, b^n(0)$
First ($n = 1$)	Linear	$\alpha = \dfrac{12}{\gamma_m}$
Second ($n = 2$)	Square	$\alpha = \dfrac{48}{\gamma_m^2}$
	Cosine	$\alpha = \dfrac{12\pi^2}{\gamma_m^2}$
Fourth ($n = 4$)	Cosine squared	$\alpha = \dfrac{90\pi^4}{\gamma_m^4}$

It is the n-th derivative which is discontinuous at the junction. For a given n-th order blending function, the discontinuity in the n-th order derivative of the radius of curvature is given by [5]

$$\epsilon_n = \frac{\alpha \, f_c \, k^{(n+3)}}{(x_m/\gamma_m)^n} \left(\frac{a_e}{(x_m/\gamma_m)} + \frac{f_c \, b_e \, k^3}{(x_m/\gamma_m)^2} - \frac{1}{2} \right) \qquad (2.40)$$

where α is a constant that depends on the type of blending function being used [5] and n is the order of the blending function. For the blending functions defined in Section 2.4, the values for α are given in Table 3. The parameters a_e, b_e, x_m, and γ_m are the blending parameters to be optimized, and k is given by

$$k = \sqrt{1 + (y_j/2f_c)^2} \, . \qquad (2.41)$$

In order to optimize the rolled edge termination, the error function given in Equation (2.40) must be minimized while still meeting the design constraints. The method of Lagrange Multipliers is used to give the following function to be

minimized [7]:

$$F = \epsilon_n^2 + \lambda_1 \left(y_t - y_{max}\right)^2 + \lambda_2 \left(\frac{R_{sh} - \lambda_{max}/4}{\lambda_{max}/4}\right)^2 , \qquad (2.42)$$

where R_{sh} is the actual radius of curvature of the blended rolled edge at the shadow boundary and y_t is the total reflector height. Also, λ_1 and λ_2 are the Lagrange multipliers for the maximum height and minimum radius of curvature in the lit region, respectively. Since it is necessary to meet the design constraints, these two terms will be heavily weighted. The terms y_{max} and $\lambda_{max}/4$ are the specified design constraints, where y_{max} is the main reflector maximum height and $\lambda_{max}/4$ is the minimum radius of curvature in the lit region of the reflector. The conjugate gradient method [14] was used to minimize the function F, thus determining the optimum blending parameters. When using the conjugate gradient method, the terms y and R_{sh} are varied until they are within a specified difference from y_{max} and $\lambda_{max}/4$. The resulting values for a_e, b_e, x_m, and γ_m are the optimized blending parameters.

Since the desired minimum is a value of zero, all the terms in Equation (2.42) have been squared to keep the minimum value of the function from going negative. Also the term associated with the radius of curvature is normalized since the radius of curvature is much smaller than the maximum height and the error term (ϵ_n). Normalizing this term will thus help to minimize the difference between R_{sh} and $\lambda_{max}/4$.

The six variables that are optimized by the conjugate gradient method for the function given by Equation (2.42) are $a_e, b_e, x_m, \gamma_m, \lambda_1$, and λ_2. It was found that the four terms a_e, b_e, x_m, γ_m are not linearly independent [7]. The γ_m term was therefore kept constant during optimization, leaving five variables to be found. In Equation (2.42), the error term, the total reflector height (y), and the radius

Table 4: Rolled edge variations with junction height (y_j)

Shadow boundary radius of curvature $= 0.1229'$				
$\gamma_m = 105°$ $f_c = 7.25'$ $r_e = 3.5'$				
y_j	a_e	b_e	x_m	error
11.5000	0.5000	2.807	10.905	19.5540
10.5000	0.5000	2.9058	10.5158	17.9886
9.5000	0.5000	3.0181	10.1974	16.3591
8.5000	0.5000	3.1344	9.9109	14.8664
7.5000	0.5000	3.2540	9.6597	13.5002
6.5000	0.5000	3.3755	9.4457	12.2666
5.5000	0.5000	3.4968	9.2711	11.1647

of curvature at the shadow boundary depend on the junction height and focal length of the parabola. Thus, the blending parameters will change with these two parameters. However, it was found that the variation in the blending parameters is not very large. This can be seen in Tables 4 and 5. The blending parameters for both tables were found using a cosine squared blending function, a minimum operating frequency of $2\,GHz$, the amount of rolled edge added was $3.5'$, and γ_m was $105°$. Table 4 shows how the blending parameters vary with the junction height, and Table 5 shows how they vary with the focal length of the reflector. The value in the error column for the two tables is found by substituting the optimized blending parameters into Equation (2.40).

The fact that the rolled edge changes with junction height will also be very important in the next chapter where three-dimensional reflectors are considered. For three-dimensional reflectors, the junction height varies continuously along the

Table 5: Rolled edge variations with focal length (f_c)

Shadow boundary radius of curvature = $0.1229'$				
$\gamma_m = 105°$ $y_j = 11.5'$ $r_e = 3.5'$				
f_c	a_e	b_e	x_m	error
7.2500	0.5000	2.807	10.905	19.5540
7.5000	0.5000	2.8285	10.7308	20.5915
8.0000	0.5000	2.8814	10.5007	22.2676
8.5000	0.5000	2.9257	10.3098	23.9617
9.0000	0.5000	2.9620	10.1514	25.6560
9.5000	0.5000	2.9910	10.0166	27.3949
10.0000	0.5000	3.0140	9.9033	29.1462

junction contour of the main reflector paraboloid. Therefore, different blending parameters will be needed as the position along the junction changes.

2.6   Blended rolled edge design example

For a two-dimensional reflector, a blended rolled edge must be designed for both the top and bottom junctions. As shown in Section 2.5, this is necessary since the junction heights are different. The same parabola used for the simple rolled edge design in Section 2.3.1 will now be used to design the top and bottom blended rolled edges. This will show the improvement in performance using the blended rolled edges. The parabola from Section 2.3.1 had a focal length of $7.25'$, the top junction at $11.5'$, the bottom junction at $5.5'$, and a maximum height of $15'$. The distance from the main origin to the target zone along the z-axis is $20'$. The difference between y_{max} and y_{top} is the amount of blended rolled edge added to the

Table 6: Surface characteristics for blended rolled edges

Shadow boundary radius of curvature $= 0.1229'$	
$\gamma_m = 105°$ $f_c = 7.25'$ $r_e = 3.5'$	
Top junction	
y_{top}	$11.5'$
a_e	$0.5'$
b_e	$2.807'$
x_m	$10.905'$
Bottom junction	
y_{bot}	$5.5'$
a_e	$0.5'$
b_e	$3.812'$
x_m	$10.088'$

parabola. From Equation (2.38), this difference gives $r_e = 3.5'$, as the amount of blended rolled edge added. The minimum operating frequency is $2\,GHz$ and cosine squared blending is used to generate the blended rolled edge. The blended rolled edge design procedure given in Section 2.5 is used to find the blending parameters. The surface characteristics and blending parameters are given in Table 6 for both the top and bottom junctions. The two-dimensional reflector with blended rolled edges is shown in Figure 9.

Figures 10 and 11 show the scattered fields from the blended rolled edge reflector. The reflector is illuminated by the Gregorian subreflector discussed in Section 2.3.1. Again the corrected PO method is used to calculate the scattered fields. The total scattered field is shown in Figure 10 and the diffracted field is
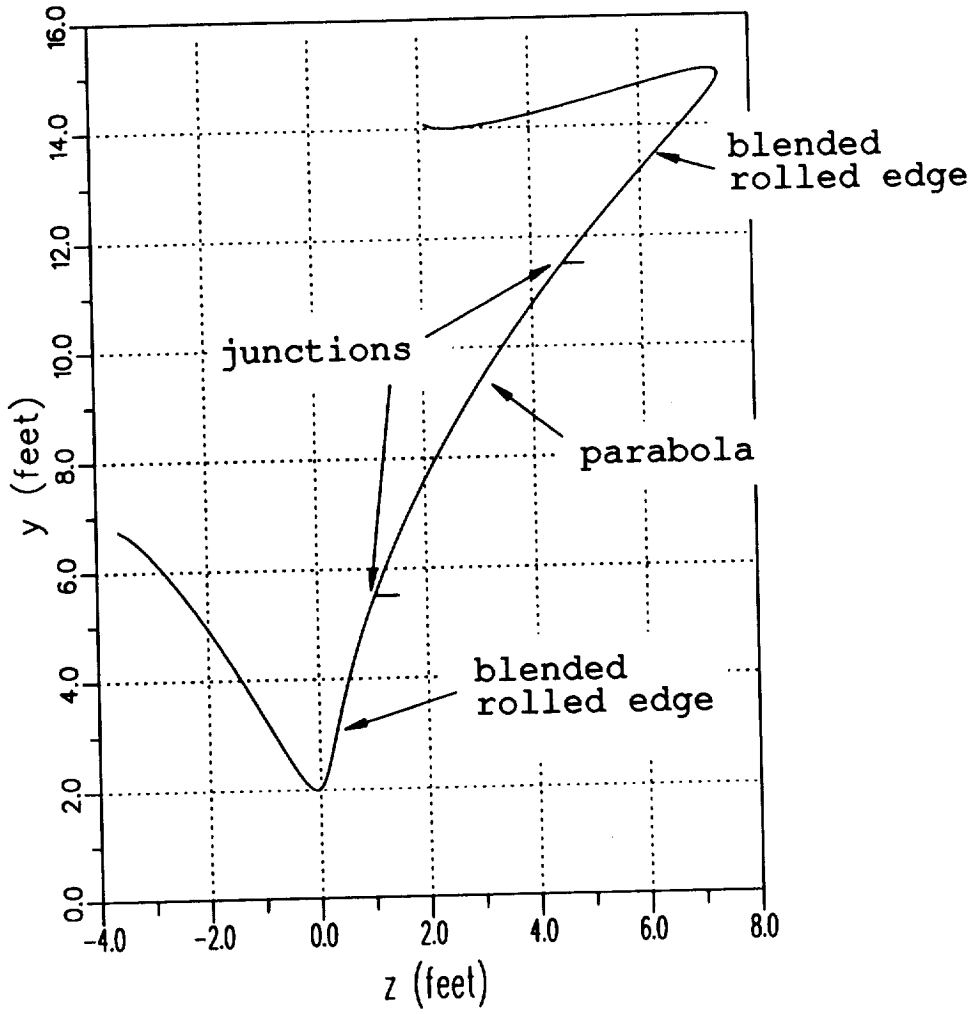
Figure 9: Two-dimensional surface with blended rolled edges.

shown in Figure 11. All fields are plotted relative to the same level for comparison.

Note that the ripple in the total scattered fields in the entire target zone is less than 0.2 dB. Thus, the size of the usable target zone is equal to the size of the reflector. The diffracted fields (Figure 11) are at least 35 dB below the GO fields. For the simple rolled edge, the diffracted fields were only 12 dB below the GO fields. Thus, the design procedure leads to a good blended rolled edge.

2.7 Summary

A procedure to design a blended rolled edge for two-dimensional reflectors was developed. The design procedure leads to a blended rolled edge that guarantees low diffracted fields and meets the constraints regarding the total height and minimum radius of curvature. First a simple rolled edge was introduced in order to develop the rolled edge (x_e, y_e) coordinate system. This coordinate system defines a plane in which the blended rolled edge is added. Note that the plane (the rolled edge plane) contains the focal point of the reflector. As shown in the next chapter, this will be important for designing a rolled edge for three-dimensional reflectors.
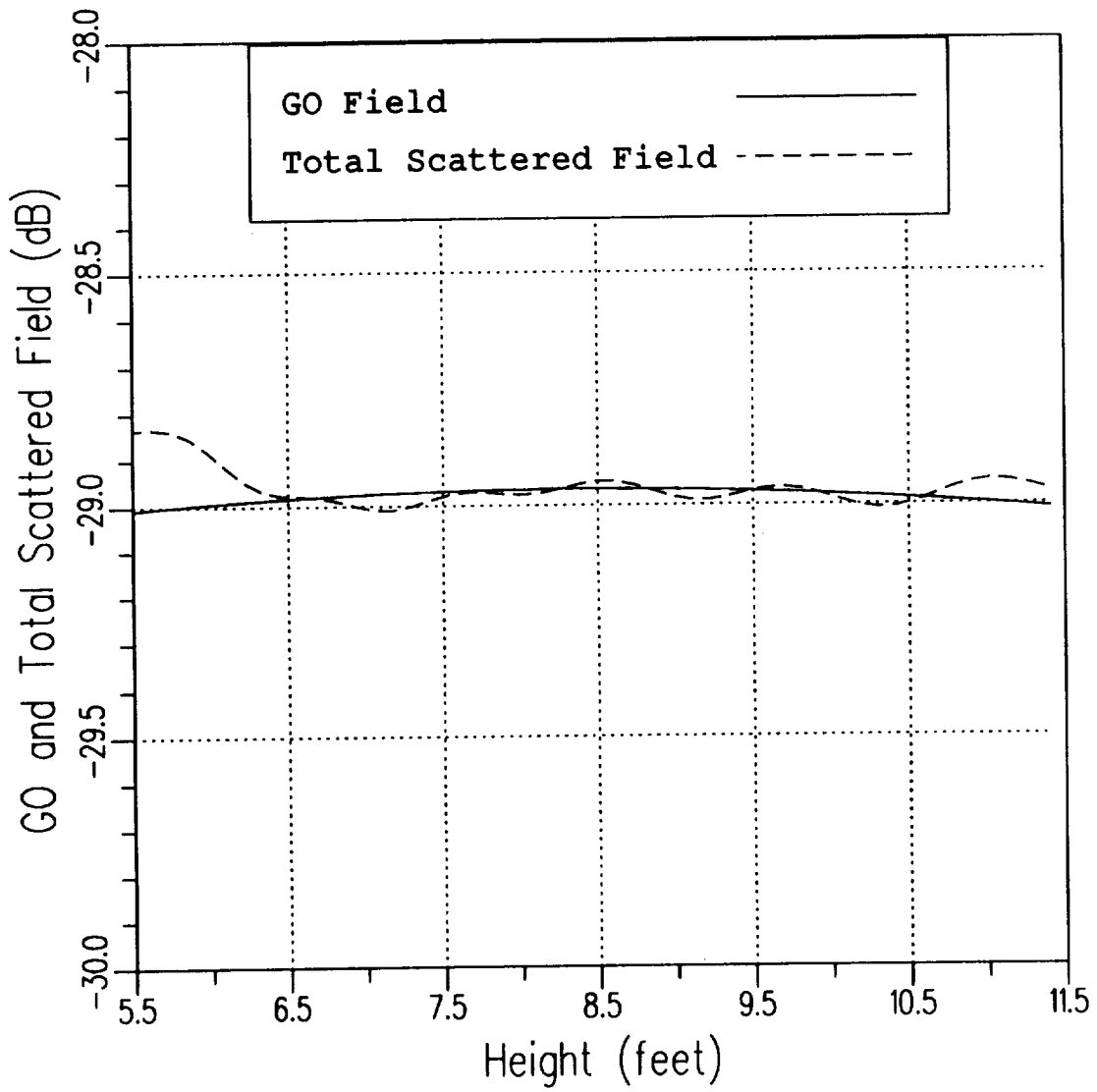
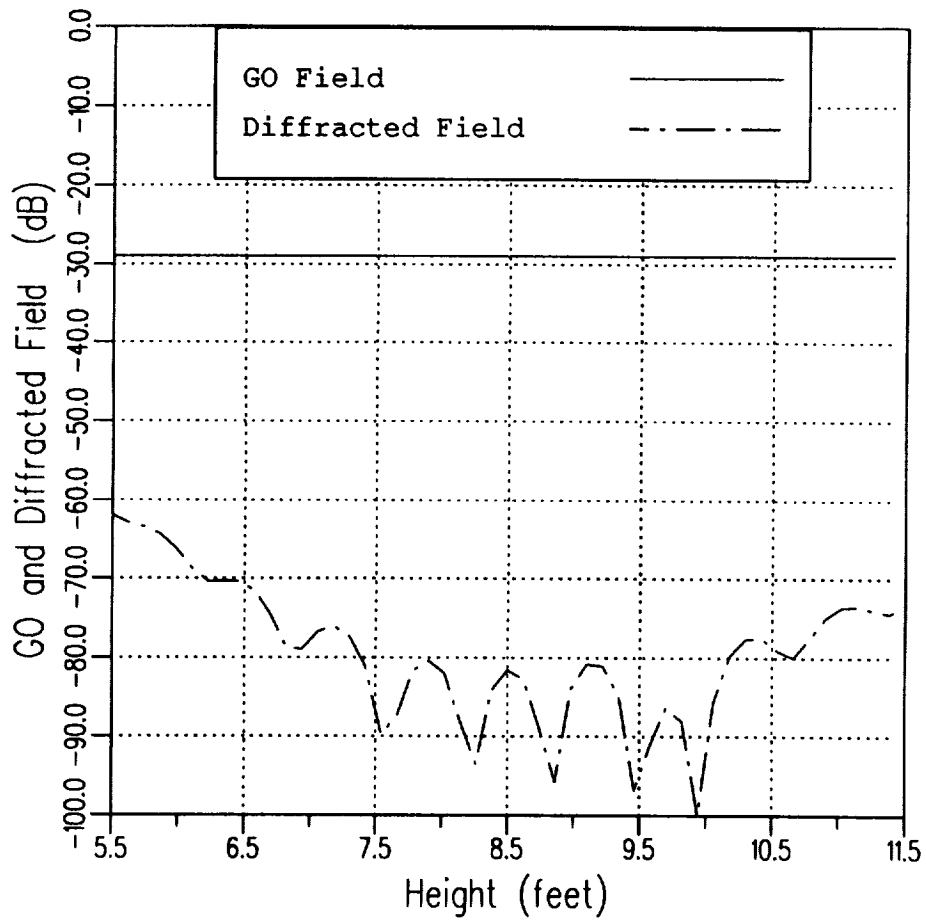Figure 10: Total scattered field 20′ from the reflector with blended rolled edges.

Figure 11: Diffracted field 20′ from the reflector with blended rolled edges.

CHAPTER III

THREE-DIMENSIONAL EDGE TREATMENT FOR THE MAIN REFLECTOR

3.1 Introduction

In this chapter the design procedure presented in Chapter II is generalized to three-dimensional main reflectors with arbitrary edge (junction) contours. For three-dimensional reflectors, it is desired that the rolled edge be added so that the surface radius of curvature is continuous across the junction. The rolled edge plane must also be chosen so that the whole surface is smooth and continuous. Finally, in order to use the design procedure outlined in the last chapter, it is necessary that the focus of the parabola and the rolled edge be in the same plane. In order to meet the first two requirements, the rolled edge plane should be chosen very carefully. Such a rolled edge plane is defined in this chapter. This rolled edge plane may not necessarily contain the focal point of the paraboloid. Therefore the concept of an equivalent parabola is introduced. The equivalent parabola has its focus in the rolled edge plane and traces the part of the three-dimensional paraboloid that lies in the rolled edge plane.

3.2 Method to add rolled edge

When adding a rolled edge to the compact range main reflector, one should make sure that the surface is smooth and continuous. In the case of blended rolled

edges, the curvature of the reflector at the junction between the rolled edge and the paraboloid should be continuous. The continuity of the surface curvature ensures that the reflected fields will be continuous across the junction. In the case of a paraboloid, the reflected wavefront is a plane wave. Thus, a blended rolled edge should be added such that the reflected wavefront just across the junction between the paraboloid and rolled edge is also planar. The reflected field is then planar on both sides of the junction. Along the junction contour (rim of the paraboloid) the reflected field caustic is at infinity, or the normal curvature of the reflected wave is zero. Thus, at a given point on the rim, the tangent to the junction contour is one principal direction (say $\hat{\tau}_2$ as shown in Figure 12) of the reflected wavefront with corresponding principal curvature (say κ_2) equal to zero. Let $\hat{\tau}_1$ be the other principal direction. Then from Euler's theorem [16] the normal curvature of the reflected wavefront in any other direction (say $\hat{t}$) is

$$\kappa = \kappa_1 \cos^2 \alpha \qquad (3.1)$$

where κ_1 is the principal curvature of the reflected wavefront in the $\hat{\tau}_1$-direction and α is the angle between $\hat{\tau}_1$ and $\hat{t}$. Let the blended rolled edge be added in a plane other than the edge plane (containing the rim tangent and the surface normal). For the rolled edge plane, $\cos^2 \alpha \neq 0$ and $\kappa = 0$. Then, from Equation (3.1), $\kappa_1 = 0$. Thus, the reflected wavefront from the rolled edge side is also planar. Note that for a smooth and continuous surface, the normal to the rolled edge at the junction contour should be continuous. Thus, the rolled edge plane should contain the surface normal. Therefore, for small diffracted fields from the junction between the rolled edge and the paraboloid, the rolled edge plane should be other than the edge plane and should contain the surface normal.

The plane of incidence is one such plane. However, consider a reflector which
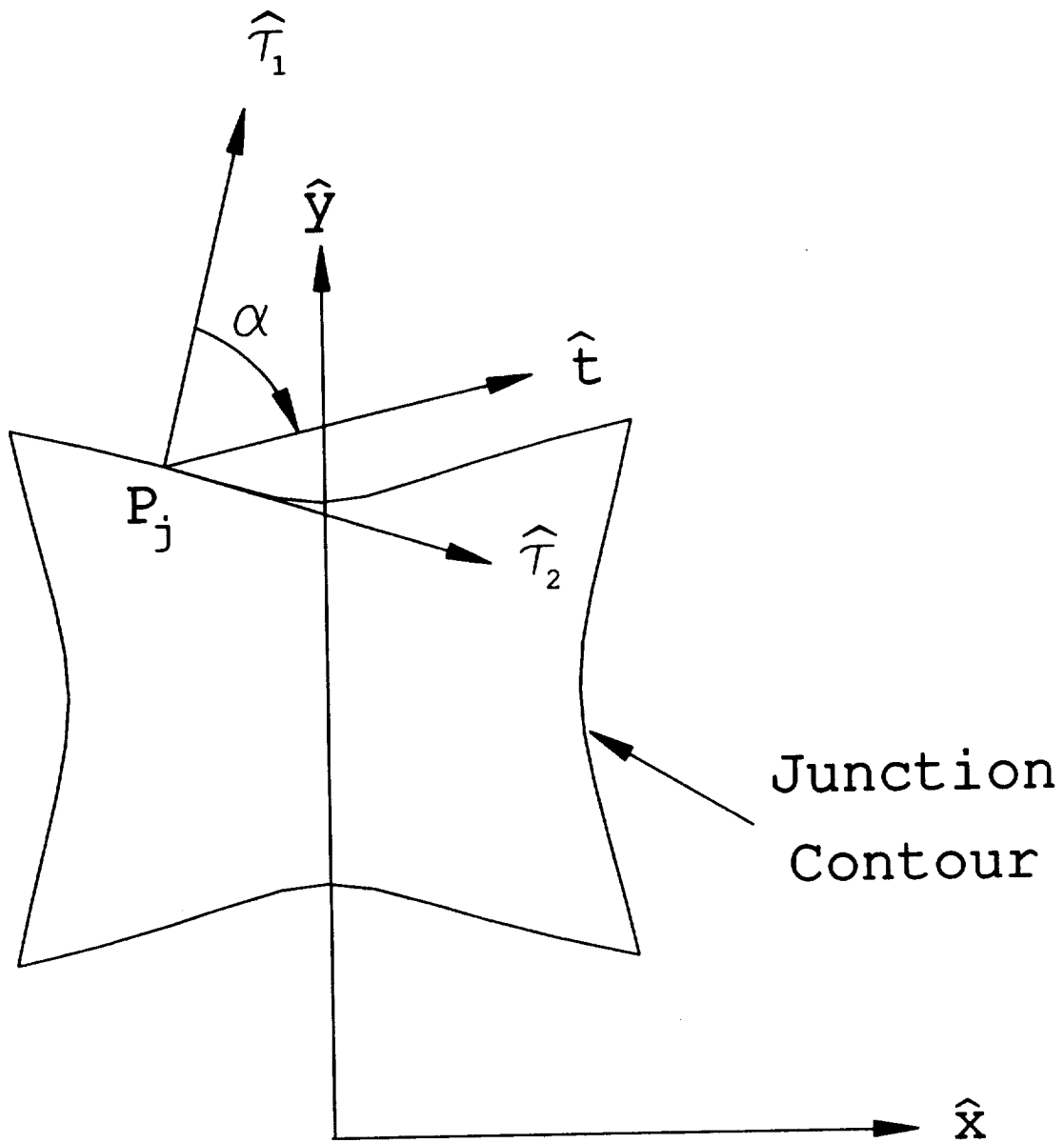
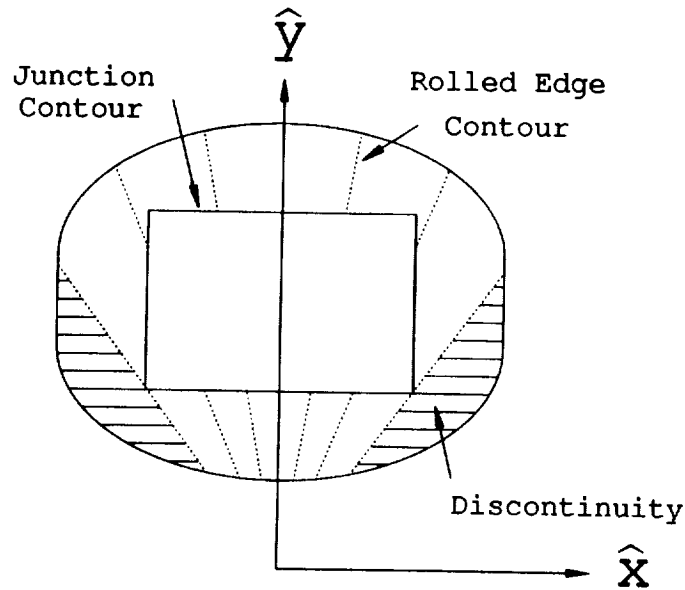Figure 12: Principal directions for the reflected wavefront.

Figure 13: Surface discontinuities caused by adding the rolled edge in the plane of incidence.

is offset such that the main origin is outside the xy-projection of the junction contour. If the rolled edge is then added in the plane of incidence, the reflector surface as shown in Figure 13 will have discontinuities at the lower end corners. If the reflector is offset such that the main origin is within the xy-projection of the junction contour, then adding the blended rolled edge in the plane of incidence will not cause any surface discontinuities. However, this would not normally be done due to the feed blockage problem. Another candidate for the rolled edge plane is a plane perpendicular to the junction contour. Note that this plane contains the surface normal too. However, adding a rolled edge in this plane will lead to a reflector surface with discontinuities along the corners as shown in Figure 14. Also, as shown in Figure 15, for arbitrary rim shapes, the rolled edge planes may intersect. Thus, the reflector surface is not defined uniquely. Therefore, the rolled
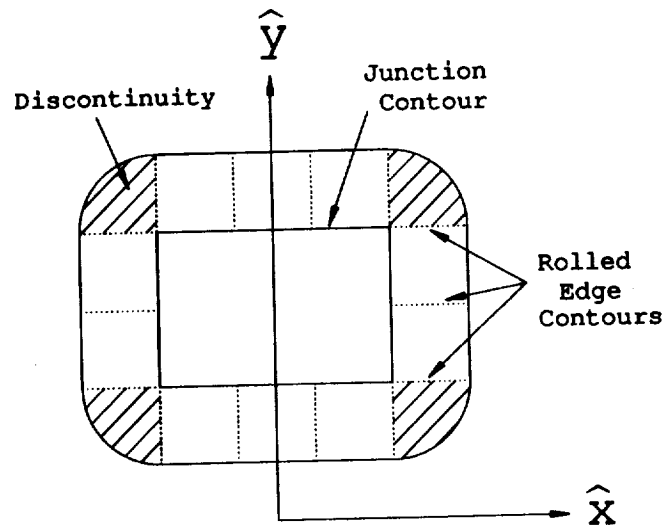
Figure 14: Surface discontinuities caused by adding the rolled edge in a plane perpendicular to the junction contour.
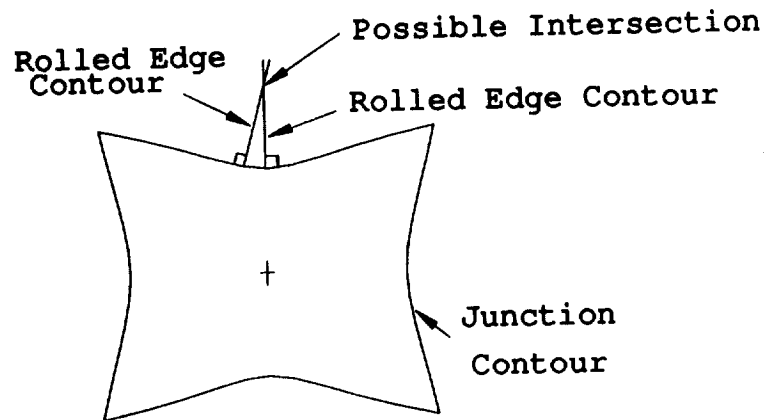

Figure 15: Intersecting rolled edge contours.

edge plane should be selected very carefully. A rolled edge plane which meets all the above requirements is defined below.

3.3 The rolled edge plane

It is first necessary to define a three-dimensional surface in which the blended rolled edge terminations can be added. Let the z-axis of the (x, y, z) cartesian coordinate system be the axis of symmetry of a paraboloid. Therefore, a paraboloid with a focal length of f_c can be described in three dimensions as

$$z = \frac{x^2 + y^2}{4f_c} .$$

(3.2)

The section of a paraboloid used for a main reflector is shown in Figure 16. The paraboloid can have any arbitrary junction contour. This arbitrary three-dimensional junction contour will then have a blended rolled edge added to it.

Let Q_j be a point on the rim of the paraboloid used as a compact range reflector. Also, let n_j be the inward normal at Q_j. Then define a vector

$$\hat{y}_e = -\hat{n}_j .$$

(3.3)

In three dimensions, the expression for the $\hat{y}_e$ unit vector is given by [5]

$$\hat{y}_e(P_j) = y_{p1}\hat{x} + y_{p2}\hat{y} + y_{p3}\hat{z}$$

(3.4)

where the coordinate values are given as

$$y_{p1} = \frac{x_j}{\sqrt{x_j^2 + y_j^2 + 4f_c^2}}$$

(3.5)

$$y_{p2} = \frac{y_j}{\sqrt{x_j^2 + y_j^2 + 4f_c^2}} , \text{ and}$$

(3.6)

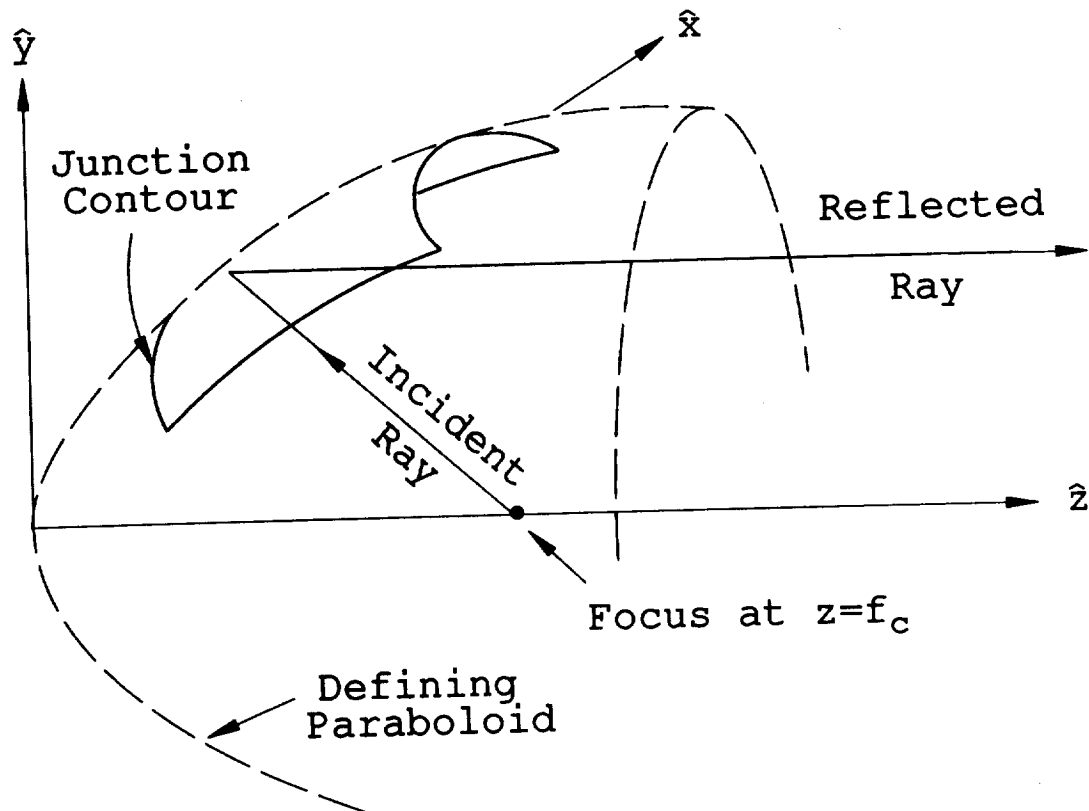$$y_{p3} = \frac{-2f_c}{\sqrt{x_j^2 + y_j^2 + 4f_c^2}} .$$

(3.7)

Figure 16: Section of paraboloid used as a main reflector.

Let P_j be the projection of the point Q_j on the (x, y) plane, and O' be the projection of the center of the reflector surface on the (x, y) plane. Then, as shown in Figure 17, define a unit vector, $\hat{\mathbf{p}}$, which is perpendicular to the radial line $\overline{O'P_j}$. Note that

$$\hat{\mathbf{p}} = p_1 \hat{\mathbf{x}} + p_2 \hat{\mathbf{y}} \tag{3.8}$$

or

$$\hat{\mathbf{p}} = \frac{-(y_j - y_{avg})}{\sqrt{(x_j - x_{avg})^2 + (y_j - y_{avg})^2}} \hat{\mathbf{x}} + \frac{x_j - x_{avg}}{\sqrt{(x_j - x_{avg})^2 + (y_j - y_{avg})^2}} \hat{\mathbf{y}} \tag{3.9}$$

where (x_j, y_j) are the coordinates of the point P_j and (x_{avg}, y_{avg}) are the coordinates of the point O'. The terms x_{avg} and y_{avg} are given by

$$y_{avg} = \frac{y_{max} + y_{min}}{2} = \frac{y_{top} + y_{bot}}{2} \text{, and} \tag{3.10}$$

$$x_{avg} = \frac{x_{max} + x_{min}}{2} = \frac{x_{rht} + x_{left}}{2} \tag{3.11}$$

where $y_{top}, y_{bot}, x_{left}$, and x_{rht} are the dimensions of the target zone as defined in the Appendix. The vector $\hat{\mathbf{p}}$ is shown in Figure 17 for both the offset and symmetric target zones. The rolled edge plane is then defined by (x_e, y_e), where

$$\hat{\mathbf{x}}_e = \frac{\hat{\mathbf{y}}_e \times \hat{\mathbf{p}}}{|\hat{\mathbf{y}}_e \times \hat{\mathbf{p}}|} = x_{p1} \hat{\mathbf{x}} + x_{p2} \hat{\mathbf{y}} + x_{p3} \hat{\mathbf{z}} \tag{3.12}$$

and the coordinate values are given by

$$x_{p1} = \frac{-y_{p3}p_2}{y_{pg}} \tag{3.13}$$

$$x_{p2} = \frac{y_{p3}p_1}{y_{pg}} \tag{3.14}$$

$$x_{p3} = \frac{y_{p1}p_2 - y_{p2}p_1}{y_{pg}} \text{, and} \tag{3.15}$$

$$y_{pg} = \sqrt{(y_{p3}p_2)^2 + (y_{p3}p_1)^2 + (y_{p1}p_2 - y_{p2}p_1)^2} \text{.} \tag{3.16}$$

Note that the (x_e, y_e) plane contains the surface normal at the junction and is different from the edge plane. Also, the xy-projection of the surface blended in the
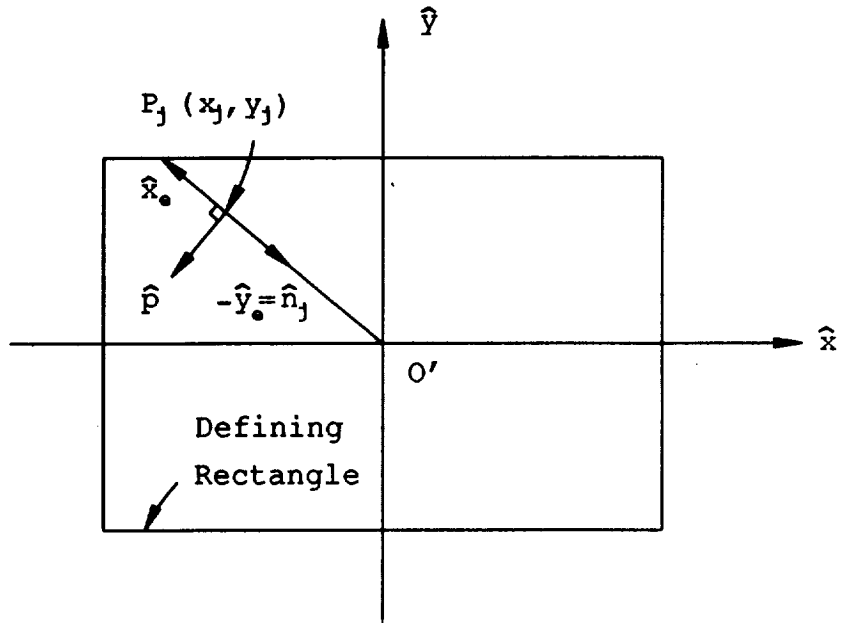
(a) Symmetric target zone
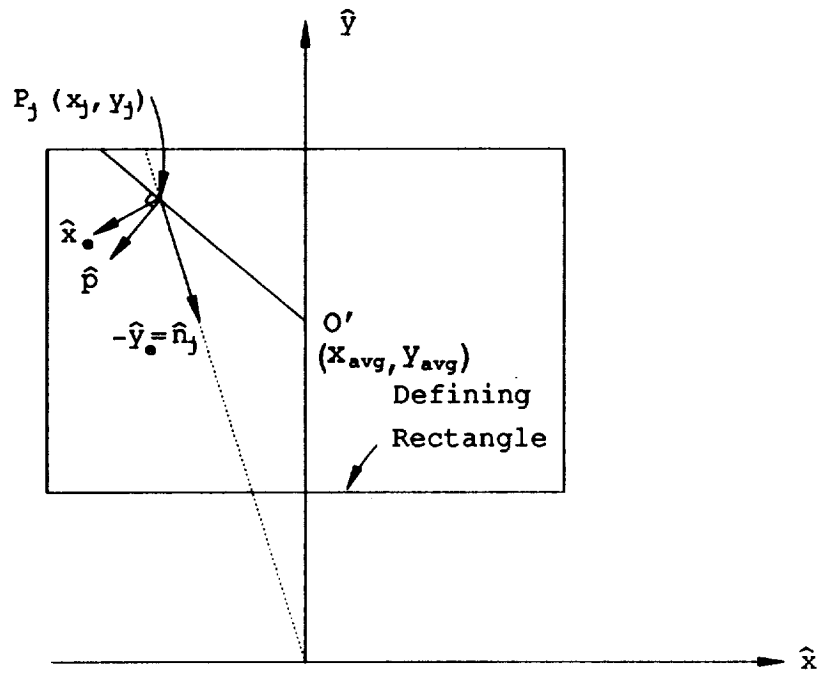
(b) Offset target zone

Figure 17: Geometry of the $\hat{p}$ vector.

41

(x_e, y_e) system will be a radial line out from the center of the reflector. Blending is done along this radial line. Thus, the blended surface is unique and continuous.

In Chapter II, a method to find the optimum blended rolled edge parameters was given. In the method, it was assumed that the focal point of the parabola lies in the rolled edge plane (two-dimensional system); however, the (x_e, y_e) plane defined above may not contain the focal point of the paraboloid. This is especially true for offset-feed reflectors. To solve this problem, one can define an equivalent parabola in the (x_e, y_e) plane. This equivalent parabola traces the part of the original paraboloid which also lies in the (x_e, y_e) plane. A simple method to find the equivalent parabola is given next.

3.4 Method to find the equivalent parabola

In order to specify the equivalent parabola, its focal length and axes should be determined. Let (y', z'), as shown in Figure 18, be the axes of the equivalent parabola and f'_c be its focal length. Since the junction point (Q') lies on the equivalent parabola and $\hat{y}_e$ is the outward normal to the paraboloid at the junction point, $\hat{y}_e$ is also normal to the equivalent parabola at Q_j. Let $\hat{x}_e$ be the tangent vector to the equivalent parabola. Then from Section 2.2.1, the transformation between the (y', z') system and the (x_e, y_e) is given by

$$
\begin{pmatrix} y'(\gamma) \\ z'(\gamma) \end{pmatrix} = \begin{pmatrix} x'_{p2} & y'_{p2} \\ x'_{p3} & y'_{p3} \end{pmatrix} \begin{pmatrix} x_e(\gamma) \\ y_e(\gamma) \end{pmatrix} + \begin{pmatrix} y'_j \\ z'_j \end{pmatrix} \tag{3.17}
$$

where (y'_j, z'_j) are the coordinates of the junction in the (y', z') system.
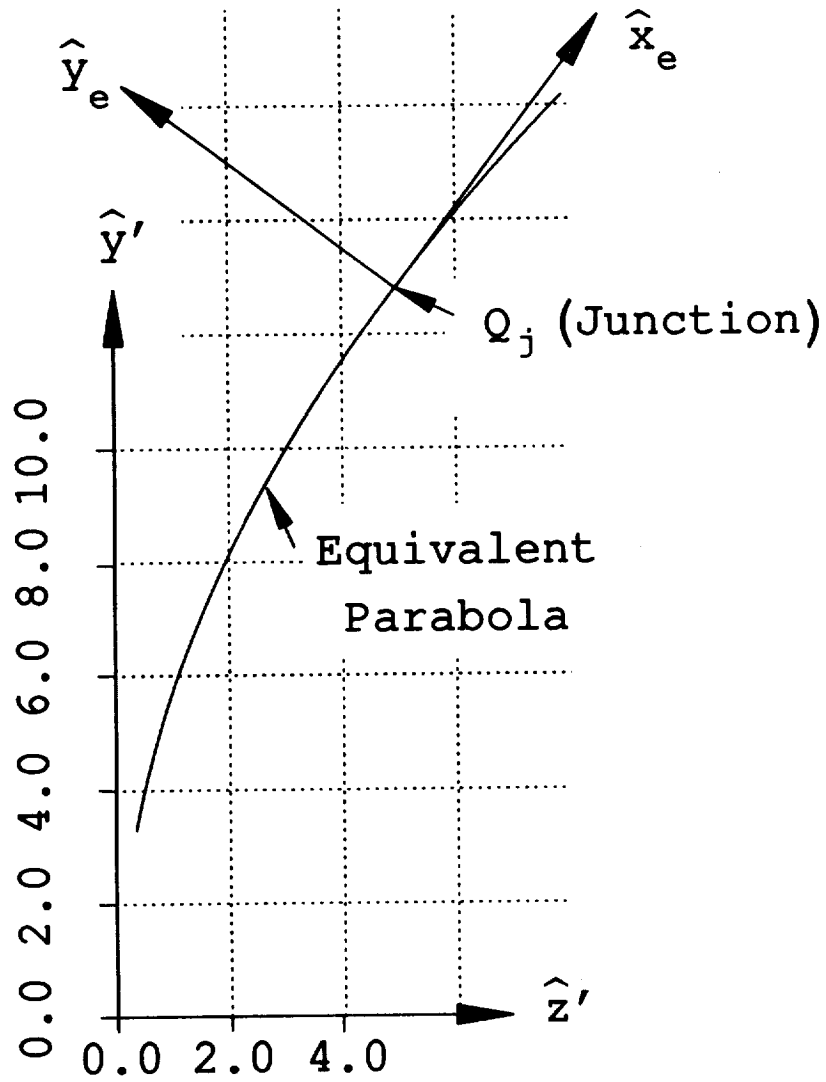
Figure 18: Equivalent parabola coordinate system (y', z').

The coordinate values for the (y', z') system are

$$y'_{p2} = \frac{y'_j}{\sqrt{(y'_j)^2 + 4(f'_c)^2}} \tag{3.18}$$

$$y'_{p3} = \frac{-2f'_c}{\sqrt{(y'_j)^2 + 4(f'_c)^2}} \tag{3.19}$$

$$x'_{p2} = -y'_{p3} \text{ , and} \tag{3.20}$$

$$x'_{p3} = y'_{p2} \text{ .} \tag{3.21}$$

Note that f'_c is the focal length of the equivalent parabola.

From the transformation given by Equation (3.17), the junction height and focal length can now be found. Substituting Equations (3.18) − (3.21) into Equation (3.17), a point (l, k) in the (x_e, y_e) system will be defined in the (y', z') system as

$$y' = \frac{2f'_c}{A}l + \frac{y'_j}{A}k + y'_j \text{ , and} \tag{3.22}$$

$$z' = \frac{y'_j}{A}l - \frac{2f'_c}{A}k + z'_j \tag{3.23}$$

where A is given as

$$A = \sqrt{(y'_j)^2 + 4(f'_c)^2} \text{ .} \tag{3.24}$$

Since the coordinate values given by Equations (3.18)− (3.21) are for the top junction, Equations (3.22) and (3.23) are thus defined with respect to the top junction. From Equation (2.1), z' is given by

$$z' = \frac{(y')^2}{4f'_c} \text{ .} \tag{3.25}$$

Equating Equations (3.23) and (3.25) gives

$$\frac{(y')^2}{4f'_c} = \frac{y'_j}{A}l - \frac{2f'_c}{A}k + \frac{(y'_j)^2}{4f'_c} \text{ .} \tag{3.26}$$

44

Next square the value y' given in Equation (3.22) and substitute the result into Equation (3.26) to give [15]

$$\left(\frac{2f_c'}{A} l + \frac{y_j'}{A} k \right)^2 + 2Ak = 0 .\qquad (3.27)$$

If the coordinate values for the bottom junction were used, the following equation must be satisfied:

$$\left(\frac{-2f_c'}{A} l + \frac{y_j'}{A} k \right)^2 + 2Ak = 0 .\qquad (3.28)$$

Equation (3.27) has two unknowns: f_c' and y_j'. Thus, by using two points on the surface of the main paraboloid that are also in the rolled edge plane, the focal length and junction height of the equivalent parabola can be found. One should know the coordinates of the two points in the (x_e, y_e) system. The coordinates of the two points in the (x_e, y_e) system can be found from the transformation [5]

$$\begin{pmatrix} x(\gamma) \\ y(\gamma) \\ z(\gamma) \end{pmatrix} = \begin{pmatrix} x_{p1} & y_{p1} \\ x_{p2} & y_{p2} \\ x_{p3} & y_{p3} \end{pmatrix} \begin{pmatrix} x_e(\gamma) \\ y_e(\gamma) \end{pmatrix} + \begin{pmatrix} x_j \\ y_j \\ z_j \end{pmatrix} \qquad (3.29)$$

where the coordinate values are given by Equations (3.5)- (3.7) and Equations (3.13) to (3.16). For a point (l, k) in the (x_e, y_e) system, Equation (3.29) gives

$$x = x_{p1} l + y_{p1} k + x_j \qquad (3.30)$$

$$y = x_{p2} l + y_{p2} k + y_j , \text{ and} \qquad (3.31)$$

$$z = x_{p3} l + y_{p3} k + z_j . \qquad (3.32)$$

Since the point (x, y, z) lies on the paraboloid, then from Equation (3.32), one obtains

$$\frac{x^2 + y^2}{4f_c} = x_{p3} l + y_{p3} k + z_j . \qquad (3.33)$$

45

Substituting Equations (3.30) and (3.31) into Equation (3.33) and then simplifying gives

$$k = \frac{-b \pm \sqrt{b^2 - 4ac}}{2a} \qquad (3.34)$$

where

$$a = y_{p1}^2 + y_{p2}^2 \qquad (3.35)$$

$$b = 2(x_{p1}\,y_{p1} + x_{p2}\,y_{p2})\,l + 2y_{p1}\,x_j + 2y_{p2}\,y_j - 4f_c\,y_{p3} \qquad (3.36)$$

and

$$c = (x_{p1}^2 + x_{p2}^2)\,l^2 + 2(x_{p1}\,x_j + x_{p2}\,y_j)\,l - 4f_c\,x_{p3}\,l \ . \qquad (3.37)$$

Thus, for a given l one can find k so that the point (l, k) lies on the paraboloid.

Since the equation for k is quadratic, there will be two solutions. To minimize numerical error when calculating f_c' and y_j', it is desired to choose the value of k that has the smallest magnitude. When this value of k is substituted into Equation (3.27), the numerical result will then have the smallest difference from zero. The value of k with the smallest magnitude is

$$k = \frac{-b + \sqrt{b^2 - 4ac}}{2a} \qquad (3.38)$$

with a, b, and c as given in Equations (3.35) − (3.37).

It is now possible to find the focus and junction of the equivalent parabola from Equation (3.27). Since this equation is a single non-linear equation of two variables, two different pair of (l, k) should be used to solve the equation. This will give two equations and two unknowns which can be solved simultaneously by Newton's Method [17]. The equivalent height and focal length along the junction contour for different reflector systems are next computed.

46

3.5 Examples of the equivalent parabola focus and junction height variation

Equation (3.27) can be solved for any type of main reflector geometry. The reflector can be either center-fed or offset-fed. The reflector can also have any arbitrary junction contour. Since the optimum parameters of a blended rolled edge depends upon the junction height and the focal length of the reflector, the equivalent height and focal length along the junction contour for various reflector systems are computed in this section. This will show the maximum variation in these parameters and will help in designing the blended rolled edge.

The center-fed systems are discussed first. The surface characteristics for the two different center-fed reflectors are given in Table 7. The different junction contours referenced in this table are formulated in the Appendix. For the center-fed system, the rolled edge plane is the same as the plane of incidence. Thus, the focal point always lies in the rolled edge plane. The first reflector considered has a circular junction as shown in Figure 19. A center-fed reflector with a circular junction contour is a body of revolution. Therefore, a center-fed reflector with a circular junction contour has no variation in the junction height or focal length of the equivalent parabola as shown in Figure 20.

The center-fed reflector with the concave junction contour is no longer a body of revolution. This type of reflector is shown in Figure 21. Although the focal length of the equivalent parabola does not change, the junction height does vary as shown in Figure 22.

The next set of reflectors considered are offset reflectors. The focus and junction height for both a circular and concave contour are found. The surface characteristics for these reflectors are given in Table 8. These reflectors have the same size target zones as the center-fed reflectors. The only difference is that they have
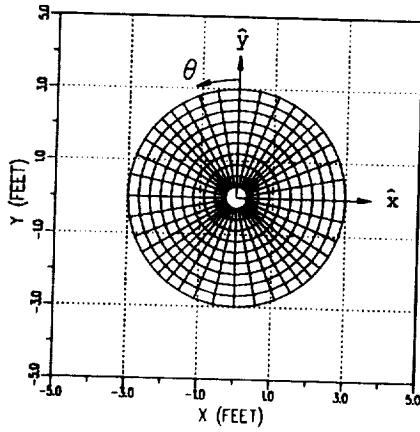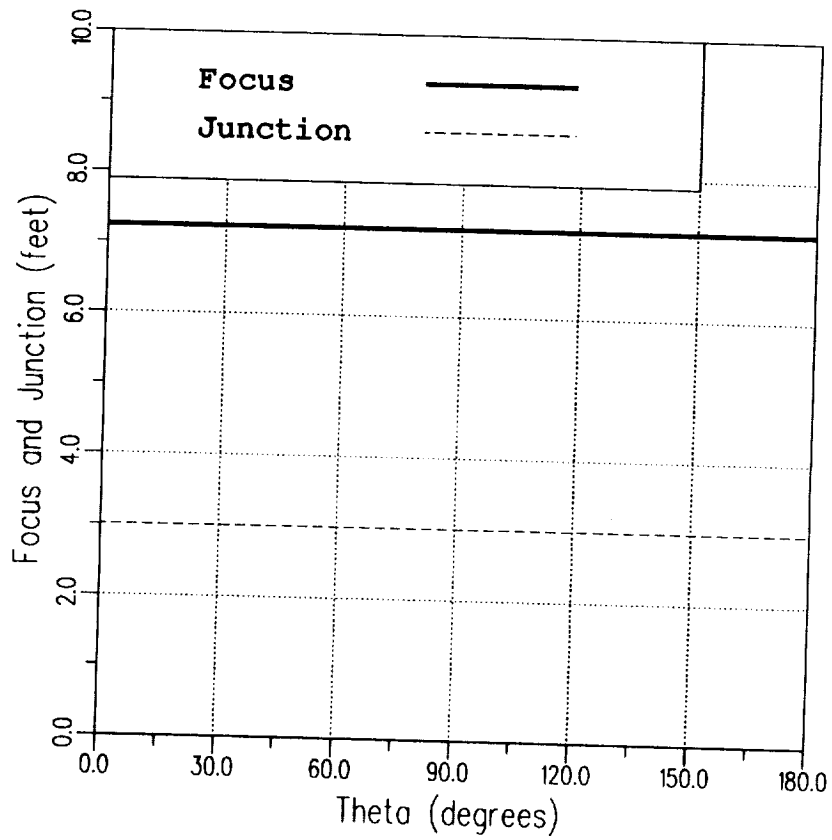
47

Figure 19: Front view of a circular rim reflector.

Figure 20: Focal length and junction height of the equivalent parabola for a circular rim, main reflector.
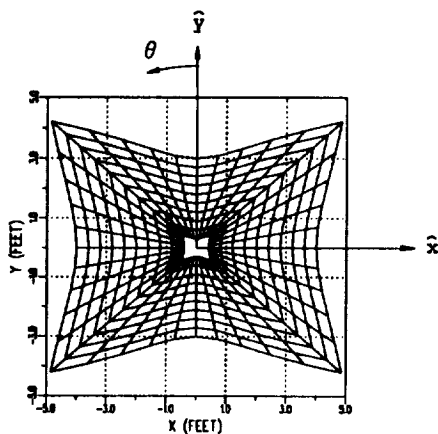
48

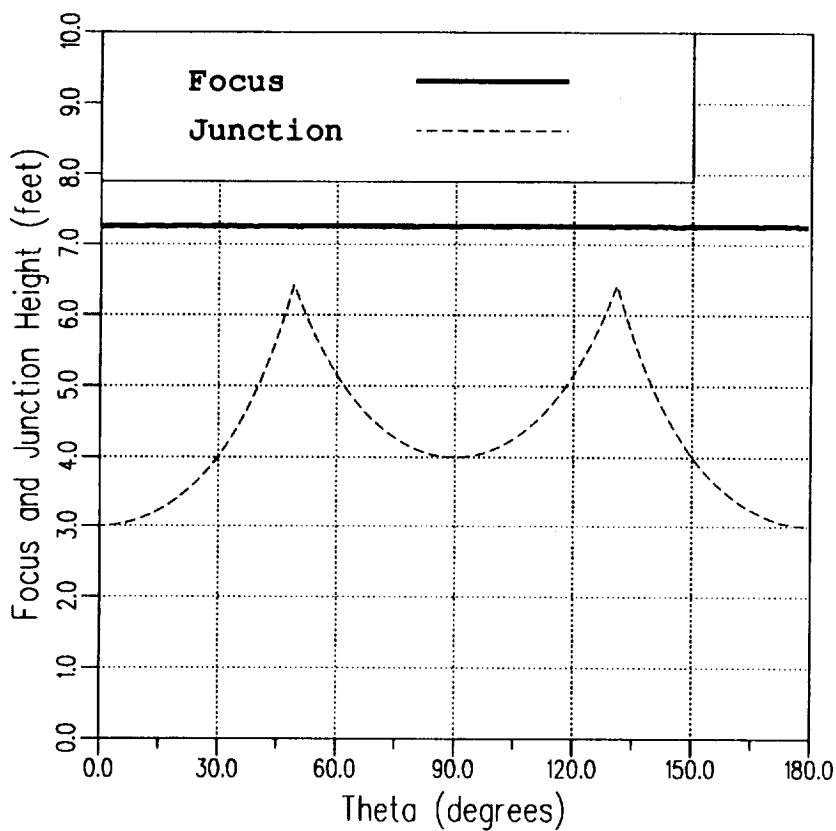**Figure 21: Front view of a concave rim reflector.**

Figure 22: Focal length and junction height of the equivalent parabola for a concave rim, main reflector.

49

Table 7: Surface characteristics for center-fed reflector examples

contour	circular	concave
f_c	$7.25'$	$7.25'$
y_{top}	$3'$	$3'$
y_{bot}	$-3'$	$-3'$
x_{left}	$-3'$	$-4'$
x_{rht}	$3'$	$4'$

Table 8: Surface characteristics for offset reflector examples

contour	circular	concave
f_c	$7.25'$	$7.25'$
y_{top}	$11.5'$	$11.5'$
y_{bot}	$5.5'$	$5.5'$
x_{left}	$-3'$	$-4'$
x_{rht}	$3'$	$4'$

been shifted up.

The focus and junction height of the equivalent parabola are shown in Figure 24 for the circular contour and in Figure 26 for the concave contour. Figure 23 shows the offset reflector with a circular junction contour while Figure 25 shows a offset reflector with a concave junction contour. As can be seen from the Figures 24 and 26, both the focus and junction height vary for the offset reflectors. This is due to the fact that for offset reflectors, the rolled edge plane is no longer the plane of incidence. Therefore, more than one set of blending parameters will be needed for these surfaces. However, since the variation is gradual, only a limited number
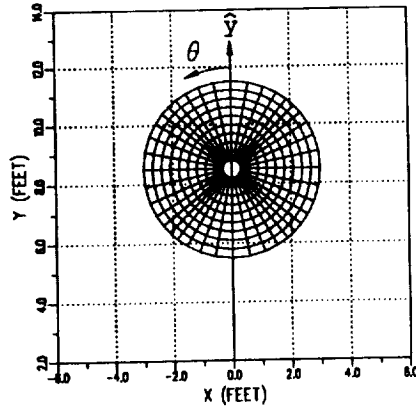
Figure 23: Front view of an offset reflector with a circular rim.

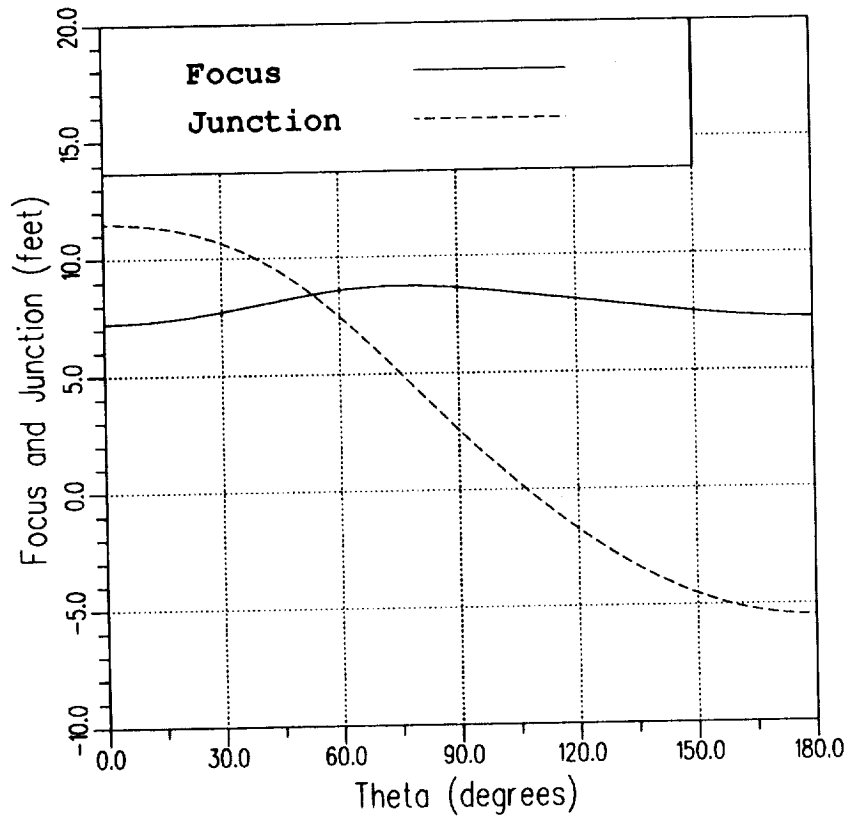**Figure 24**: Focal length and junction height of the equivalent parabola for an offset, circular rim, main reflector.
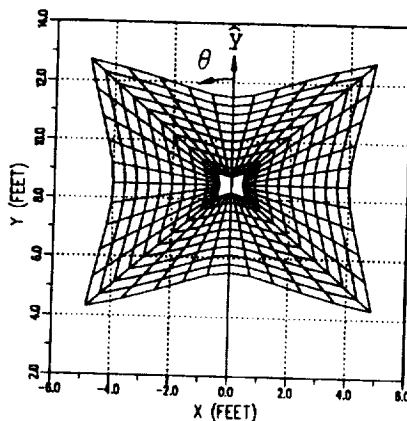
51

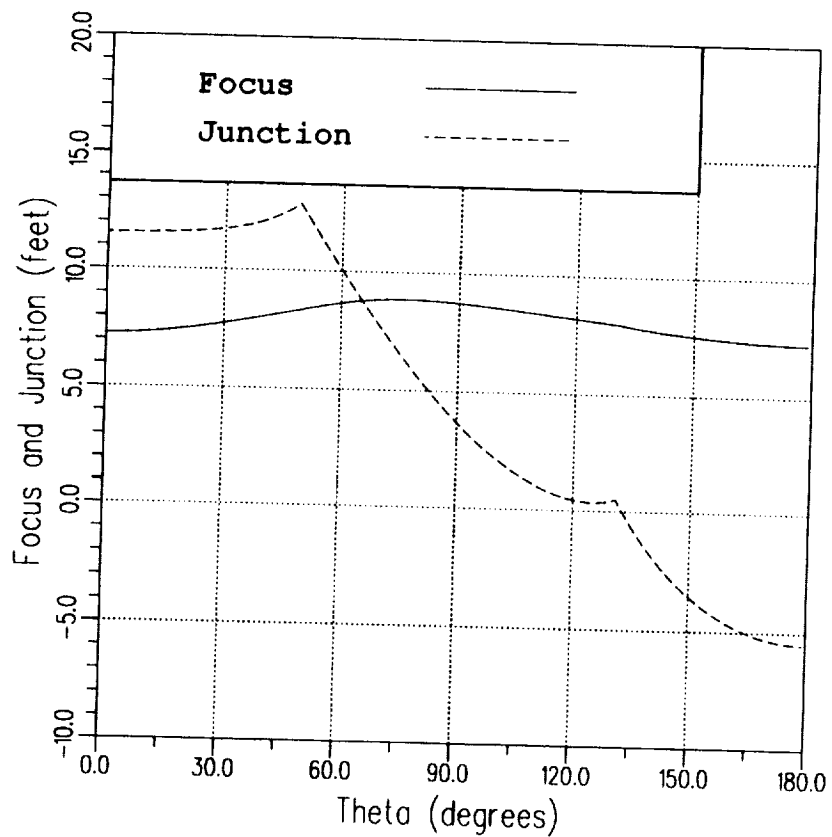Figure 25: Front view of an offset reflector with a concave rim.

Figure 26: Focal length and junction height of the equivalent parabola for an offset, concave rim, main reflector.
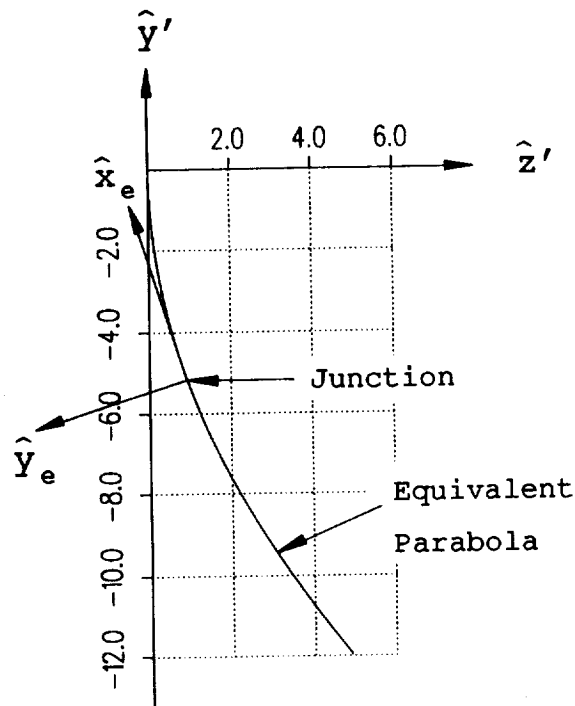
Figure 27: Equivalent parabola with a negative junction height.

of equivalent parabolas and their corresponding blending parameters are required.

The negative value for some of the junction heights is due to the fact that the top junction equation is used to find the equivalent parabola. This was shown in Section 3.4. Figure 27 shows an example of the equivalent parabola and the position of the junction when the junction height is negative.

Now that an equivalent parabola can be found, a complete design procedure can be outlined. This procedure is given in the next section.

3.6 Design procedure for a blended rolled edge

In order to design a blended rolled edge for a compact range main reflector, certain physical quantities about the paraboloid must be specified. Specifying these quantities will be the first step in the overall design procedure which follows:

1. Specify the paraboloid focus (f_c), the minimum operating frequency (f_{min}), the maximum dimensions of the reflector $(y_{max}, y_{min}, x_{max}, x_{min})$, and the dimensions of the target zone $(y_{top}, y_{bot}, x_{left}, x_{rht})$.

2. Select a blending function.

3. For a given point on the junction contour, find the rolled edge plane. This is the (x_e, y_e) plane as developed in Section 3.3.

4. Find the junction height and focal length of the equivalent parabola in the plane of the rolled edge. This procedure is given in Section 3.4.

5. Use the design procedure given in Section 2.5 to find the optimum rolled edge parameters for the given point on the junction contour.

6. Add the blended rolled edge to the equivalent parabola in the equivalent parabola coordinate system. This is the (y', z') system as defined in Section 3.4.

7. Transform each blended rolled edge back to the main (x, y, z) coordinate system in order to regenerate the complete main reflector.

The method to transform the blended rolled edge coordinates from the equivalent parabola system (y', z') to the main coordinate system (x, y, z) is given next.

3.7 Transformation from the equivalent parabola system to main coordinate system

To transform the blended rolled edge optimized in the (y', z') system to the main (x, y, z) system, first solve Equation (3.17) for (x_e, y_e). This gives

$$\begin{pmatrix} x_e \\ y_e \end{pmatrix} = \begin{pmatrix} x'_{p2} & y'_{p2} \\ x'_{p3} & y'_{p3} \end{pmatrix} \begin{pmatrix} y' - y'_j \\ z' - z'_j \end{pmatrix} . \tag{3.39}$$

The coordinate values $(x'_{p2}, x'_{p3}, y'_{p2}, y'_{p3})$ are the same as given in Equations (3.18) to (3.21). The terms y' and z' are the expressions for the optimized blended rolled edge in the (y', z') system. Next, substitute Equation (3.39) into Equation (3.29) to give

$$\begin{pmatrix} x \\ y \\ z \end{pmatrix} = \begin{pmatrix} x_{p1} & y_{p1} \\ x_{p2} & y_{p2} \\ x_{p3} & y_{p3} \end{pmatrix} \begin{pmatrix} x'_{p2} & y'_{p2} \\ x'_{p3} & y'_{p3} \end{pmatrix} \begin{pmatrix} y' - y'_j \\ z' - z'_j \end{pmatrix} + \begin{pmatrix} x_j \\ y_j \\ z_j \end{pmatrix} . \tag{3.40}$$

This is the desired transformation from the (y', z') system to the (x, y, z) system. Since the blending is done in the (y', z') system, the expressions for y' and z' are needed. These expressions can be found using Equations (2.36) and (2.37) and are given below:

$$\begin{aligned} y'(\gamma) &= \left[\gamma \left(\frac{x_m}{\gamma_m} \right) x'_{p2} + y'_j \right] [1 - b(\gamma)] \\ &\quad + [(a_e \sin \gamma) x'_{p2} + b_e(1 - \cos \gamma) y'_{p2} + y'_j] b(\gamma) \end{aligned} \tag{3.41}$$

and

$$\begin{aligned} z'(\gamma) &= \left(\frac{[\gamma(x_m/\gamma_m) x'_{p2} + y'_j]^2}{4 f'_c} \right) [1 - b(\gamma)] \\ &\quad + [(a_e \sin \gamma) x'_{p3} + b_e(1 - \cos \gamma) y'_{p3} + z'_j] b(\gamma) \end{aligned} \tag{3.42}$$

where a_e, b_e, x_m, and γ_m are the optimum blending parameters in the (y', z') system.

Equation (3.40) is then used to transform each optimized rolled edge from the local (y', z') system to the (x, y, z) system. In the (x, y, z) system, each optimized rolled edge is then added to the corresponding junction point of the three-dimensional reflector. The procedure given in this section can now be used to design a blended rolled edge for a compact range main reflector. Design examples using this procedure are given in the next section.

3.8 Three-dimensional blended rolled edge design examples

The design procedure given in the previous section is now used to design an optimum blended rolled edge for the two offset reflectors discussed in Section 3.5. For both reflectors, the minimum operating frequency is $2\,GHz$, the focal length is $7.25'$, and cosine squared blending is used to generate the blended rolled edge. The height of the rolled edge added to both reflectors is selected to be $3.5'$. Therefore, r_e is equal to $3.5'$. The formulation of the different junction contours is given in the Appendix. The equations for the dimensions of the target zone and maximum reflector size are also given in this Appendix. From Equations (A.1)-(A.4) in the Appendix and the target zone dimensions given in Table 8, the dimensions of the defining rectangle for the concave junction contour reflector are:

$$y_{max} = 15'$$
$$y_{min} = 2'$$
$$x_{max} = 7.5' \text{ , and}$$
$$x_{mim} = -7.5' \text{ .}$$

56

Using Equations (A.11)-(A.14) in the Appendix, the maximum dimensions of the circular junction contour reflector are:

$$y_{max} = 15'$$
$$y_{min} = 2'$$
$$x_{max} = 6.5' , \text{ and}$$
$$x_{mim} = -6.5' .$$

The xy-projection of the maximum dimensions of the reflector with the concave junction contour forms a rectangle of the same dimensions as the defining rectangle. The xy-projection of the maximum dimensions of the reflector with a circular junction contour forms a circle.

Tables 9 and 10 give the optimum blending parameters for the two reflectors. Note that the optimum blending parameters are given for a few points on the rim of the reflector. For other points on the rim, the blending parameters were found by interpolating these values. Since the junction height and focal length of the equivalent parabola has slow variation, the interpolation gives a very good approximation. The focal length and the junction height of the equivalent parabolas are also given in the tables.

The reflectors with optimum blended rolled edges generated using the blending parameters from Tables 9 and 10 are shown in Figures 28 to 32 for various view angles. The bold line in the plots of the surfaces indicates the junction contour between the paraboloid and the blended rolled edge. As can be seen from Figure 30, the xy-projection of the reflector with a concave junction contour has exactly the same dimensions as the defining rectangle.

Figure 33 shows the concave rim reflector where the blended rolled edge is generated from a single set of blending parameters. The blending parameters for
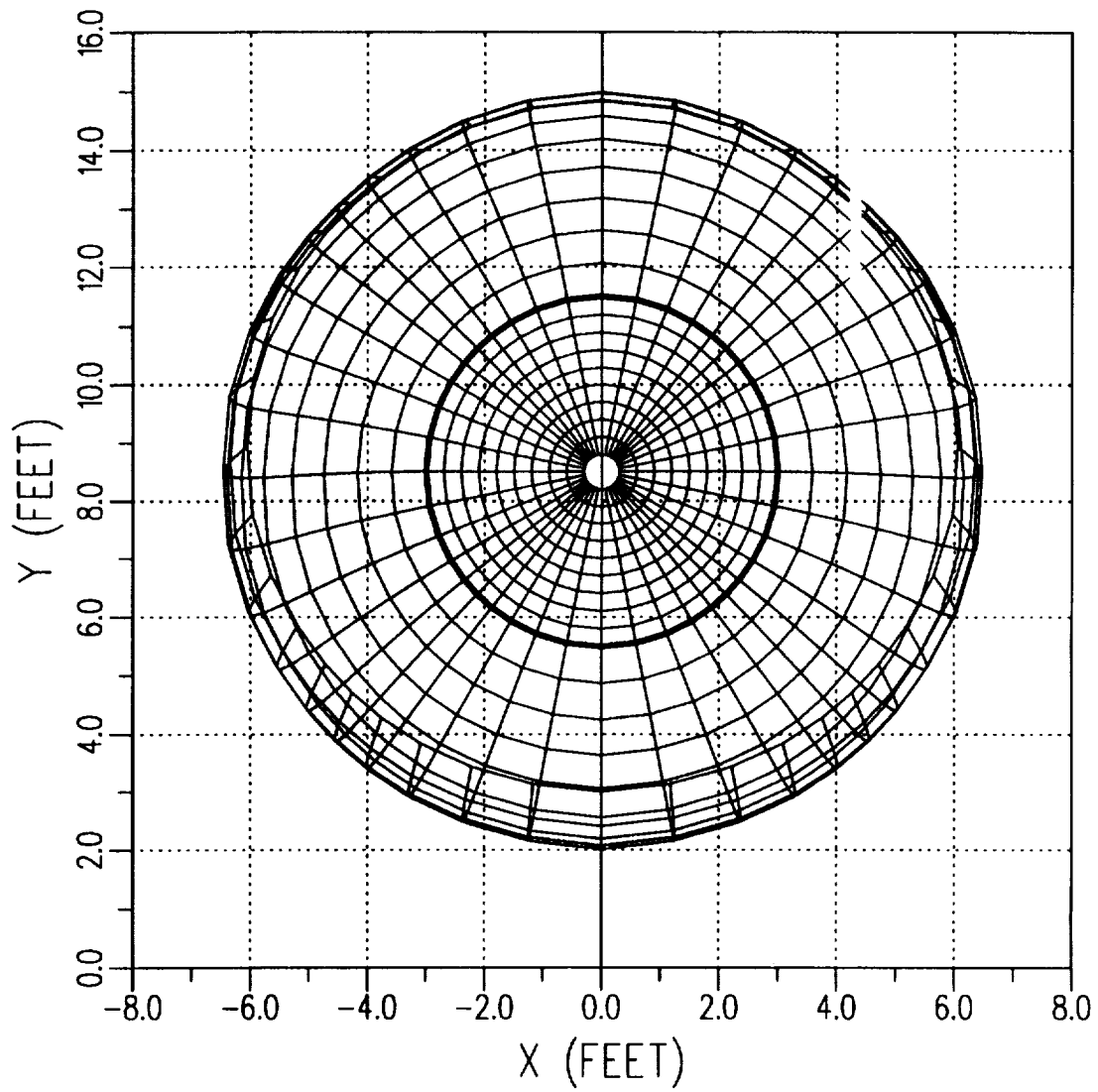
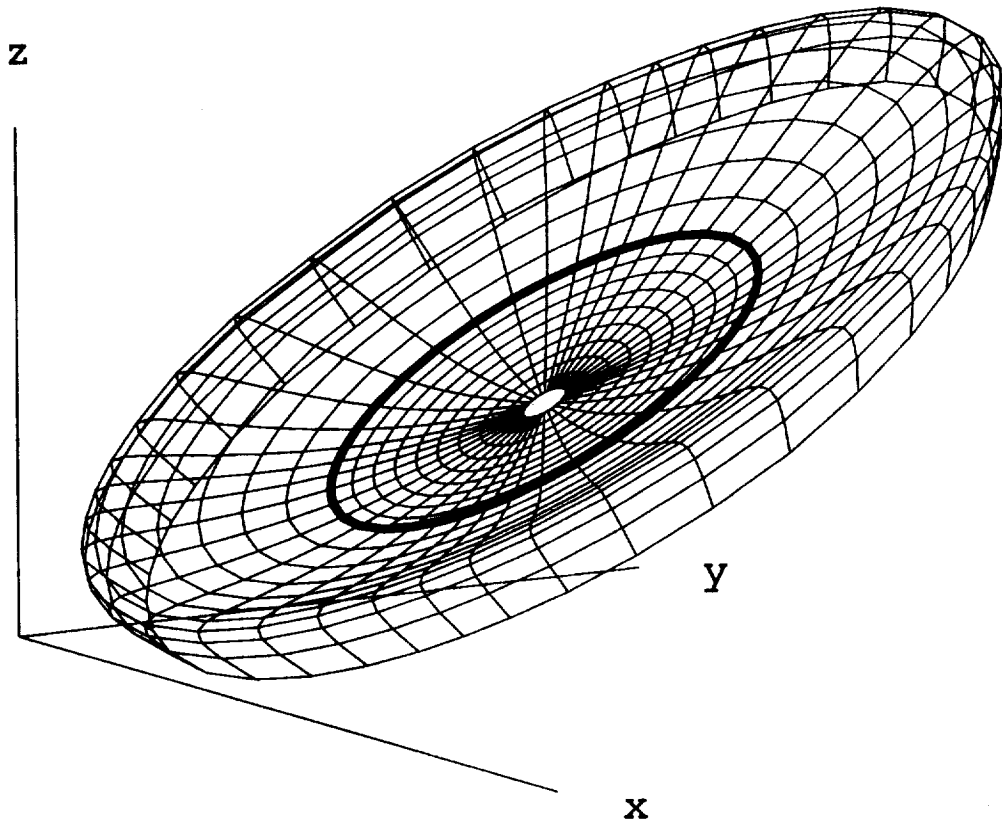Figure 28: Blended rolled edge added to a circular junction contour (Front view).

Figure 29: Blended rolled edge added to a circular junction contour (View angle: $\theta = 80°, \phi = -30°$).
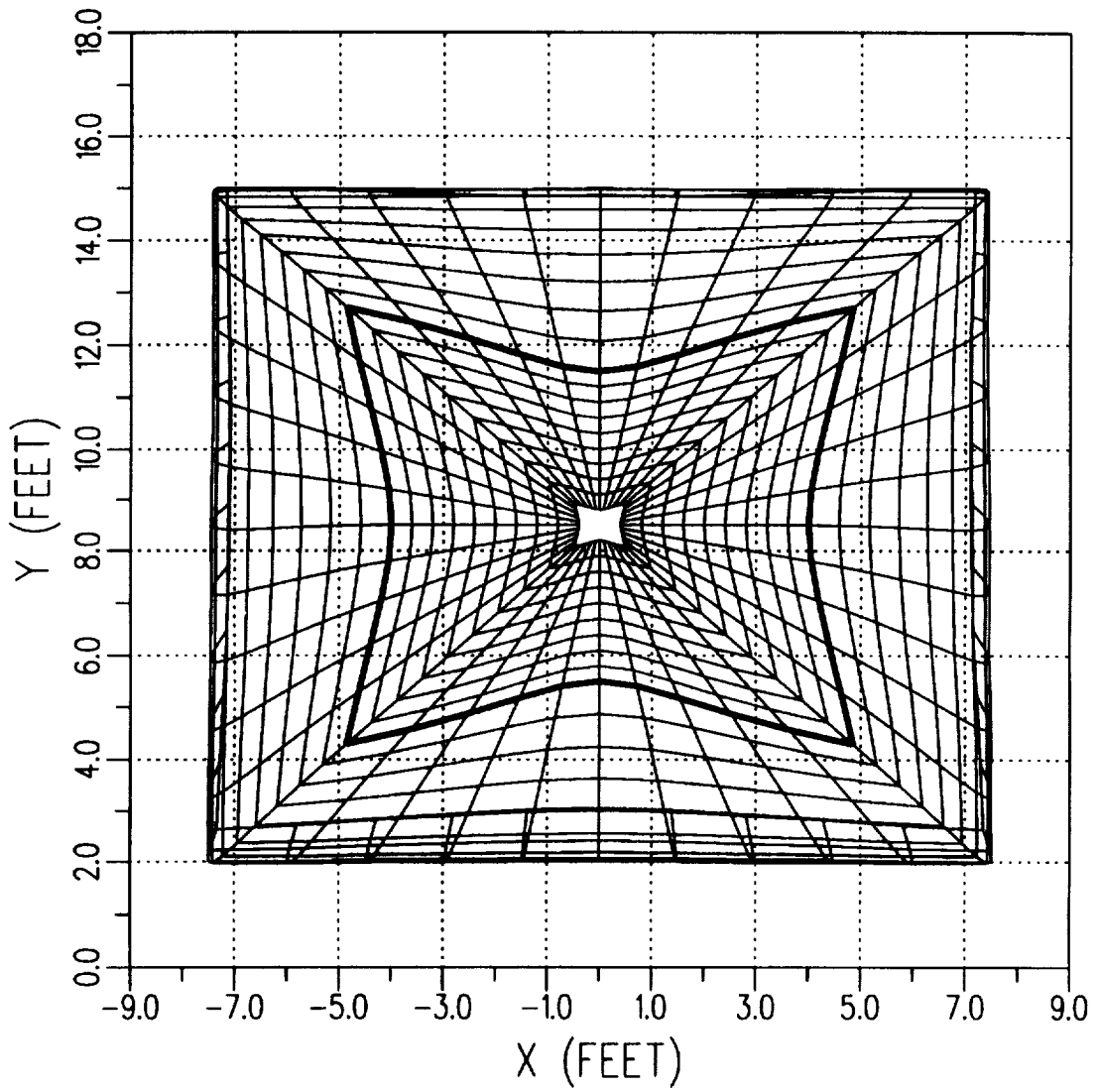
Figure 30: Blended rolled edge added to a concave junction contour (Front view).
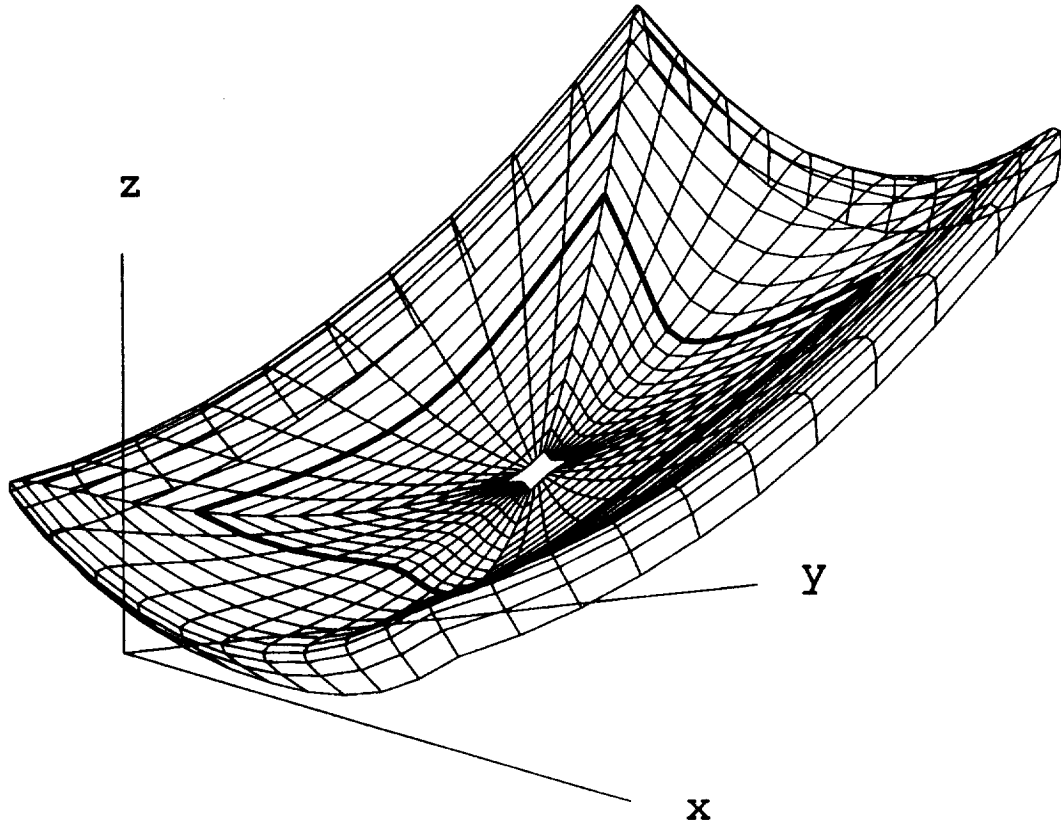
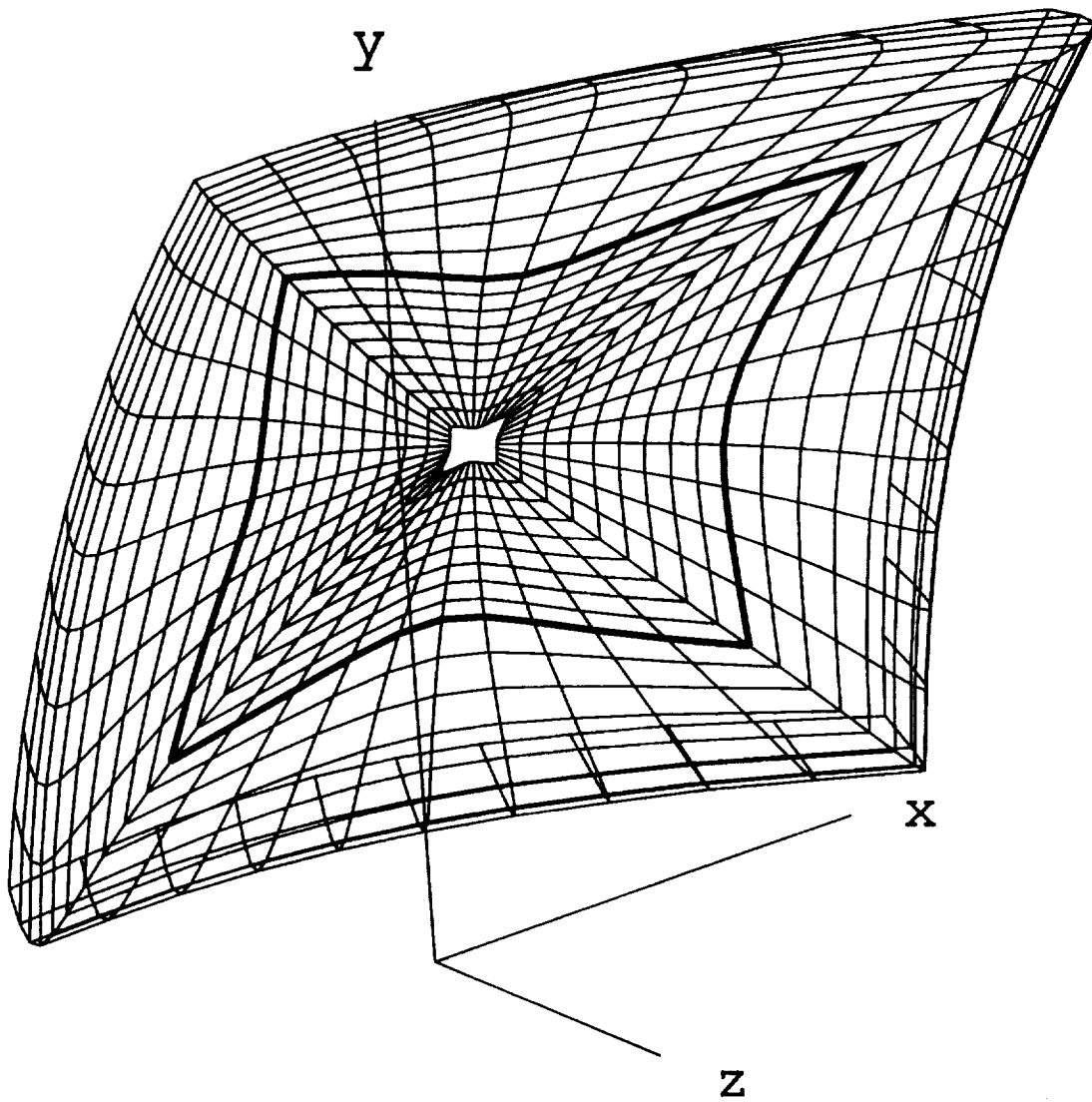Figure 31: Blended rolled edge added to a concave junction contour (View angle: $\theta = 80°, \phi = -30°$).

Figure 32: Blended rolled edge added to a concave junction contour (View angle: $\theta = 30°, \phi = 150°$).

Table 9: Optimum rolled edge parameters for a circular junction contour

θ	f_c'	y_j'	a_e	b_e	x_m	error
Shadow boundary radius of curvature $= 0.1229'$						
$\gamma_m = 105°$ $r_e = 3.5'$						
0°	7.2500	11.5000	0.5000	2.7983	10.8637	19.7561
15°	7.3800	11.3000	0.5000	2.8351	10.7234	19.8224
45°	8.2000	9.4000	0.5000	3.0998	9.8753	19.0642
90°	8.6500	2.5500	0.5000	3.6330	9.0019	11.7892
120°	8.1100	−1.7100	0.5000	3.8029	9.2251	8.5386
150°	7.5400	−4.5300	0.5000	3.8084	9.7680	7.3133
180°	7.2500	−5.5000	0.5000	3.7972	10.0721	6.9793

this surface are for $\theta = 0°$ from Table 10.

From Figure 33, the surface using a single set of blending parameters is larger than the desired defining rectangle. Usually, the maximum dimensions for a reflector are chosen so that the reflector will fit in a specified room while leaving space between the room walls and the reflector for any necessary absorber material. This is how the defining rectangle dimensions are found. Therefore, a reflector with a blended rolled edge generated from a single set of blending parameters may be too large to fit in the required space. Being able to exactly specify the dimensions of the main reflector is another advantage to using multiple sets of blending parameters to generate the blended rolled edge.

Table 10: Optimum rolled edge parameters for a concave junction contour

| Shadow boundary radius of curvature = 0.1229′ $\gamma_m = 105°$ $r_e = 3.5′$						
θ	f_c'	y_j'	a_e	b_e	x_m	error
0°	7.2500	11.5000	0.5000	2.8070	10.9050	19.3173
30°	7.7300	11.7200	0.5000	2.8410	10.7300	21.3239
49.09°	8.3100	12.8300	0.5000	2.7990	10.8090	25.5636
60°	8.6600	10.0400	0.5000	3.0750	9.9400	21.2228
75°	8.8600	6.5600	0.5000	3.3810	9.2970	16.4578
90°	8.7500	3.6600	0.5000	3.5840	9.0650	12.7710
105°	8.4900	1.5700	0.5000	3.6660	8.8980	11.5010
120°	8.2000	0.4500	0.5000	3.8050	9.0610	9.3977
130°	7.9800	0.4900	0.5000	3.8490	9.0640	8.9273
145°	7.6300	−2.7500	0.5000	3.9120	9.3820	7.6514
157°	7.4300	−4.3700	0.5000	3.8640	9.7610	7.0979
168°	7.3000	−5.2000	0.5000	3.8320	9.9990	6.9596
180°	7.2500	−5.5000	0.5000	3.8120	10.0880	6.9420
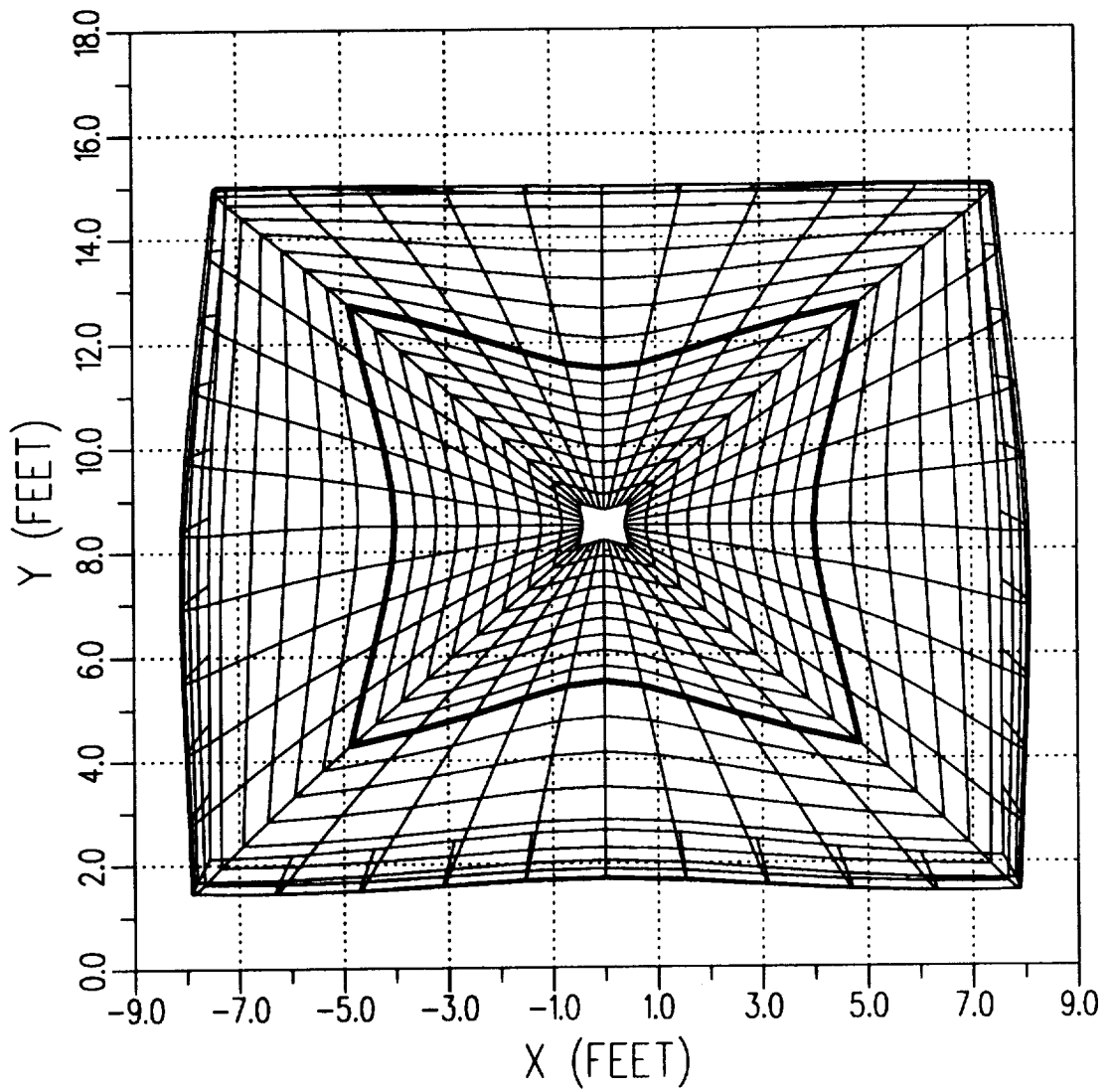
Figure 33: Paraboloid with a blended rolled edge generated from a single set of blending parameters (Front view).

3.9 Summary

In this chapter a method to design blended rolled edges for three-dimensional, compact range, main reflectors was presented. The method leads to a smooth and continuous reflector and is applicable to center-fed as well as offset-fed reflectors with arbitrary junction contours. The design procedure also guarantees that the reflector will fit inside the given dimensions. Performance of a reflector designed using the above method is discussed in the next chapter.

CHAPTER IV

PERFORMANCE OF OPTIMIZED COMPACT RANGE REFLECTORS

4.1 Introduction

In this chapter, the scattered fields from offset-fed concave junction reflectors in the target zone are discussed. The concave edge reflector with a blended rolled edge generated from a fixed set of blending parameters (see Figure 33) and the reflector with a blended rolled edge generated from a varying set of blending parameters (see Figure 30) are studied. It is shown that the reflector with the varying blended rolled edge provides improved performance. The total scattered fields and the diffracted fields from both types of reflectors are computed. This way, the improvement resulting from the blended rolled edge with varying blending parameters can be easily observed. The subreflector system configuration described in Section 2.3.1 is used for these three-dimensional reflectors. Since these reflectors are three-dimensional, the primary feed antenna will no longer be a line source. For these examples, a y-polarized, Huygen's point source with unit amplitude is used as the primary feed antenna. The operating frequency is $2\,GHz$, and the distance from the reflector to the target zone is $20'$.

67

4.2 Scattered fields along vertical cuts

Figure 34 shows the scattered fields in the target zone along a vertical cut with the horizontal displacement (x) equal to zero. The total scattered field as well as the GO component of the total scattered field for both reflectors are plotted. Since in the target zone, the GO fields are due to the parabolic section of the reflector, both reflectors have the same GO scattered fields. Note that the total scattered fields of both reflectors oscillate around the GO scattered fields. These oscillations are due to the diffracted fields from the junction between the paraboloid and the blended rolled edge. The ripple of the oscillations for the reflector with the fixed blending parameters is slightly larger than that for the optimized rolled edge (varying blending parameters). Thus, the diffracted field level for the non-optimized rolled edge (fixed blending parameters) is slightly higher than that for the optimized rolled edge. This can be seen in Figure 35 where the diffracted fields for the two reflectors are plotted. The diffracted fields were obtained by subtracting the GO fields from the total scattered fields.

All field components are plotted relative to the same level for comparison. Note that for both reflectors, the diffracted fields are at least $30\,dB$ below the GO fields. Also, note that the diffracted fields shown in Figure 35 are slightly higher than the diffracted fields for the two-dimensional case shown in Figure 11. This is due to the fact that the two side-junction contours are causing diffracted fields in the target zone of the three-dimensional reflector.

Figure 36 shows the scattered fields in the target zone along a vertical cut when the horizontal displacement is $3'$. This cut is $1'$ away from the junction contour. Therefore this cut shows the performance of the reflector close to the edge of the target zone. Also, since these reflectors are symmetric about $x = 0$,
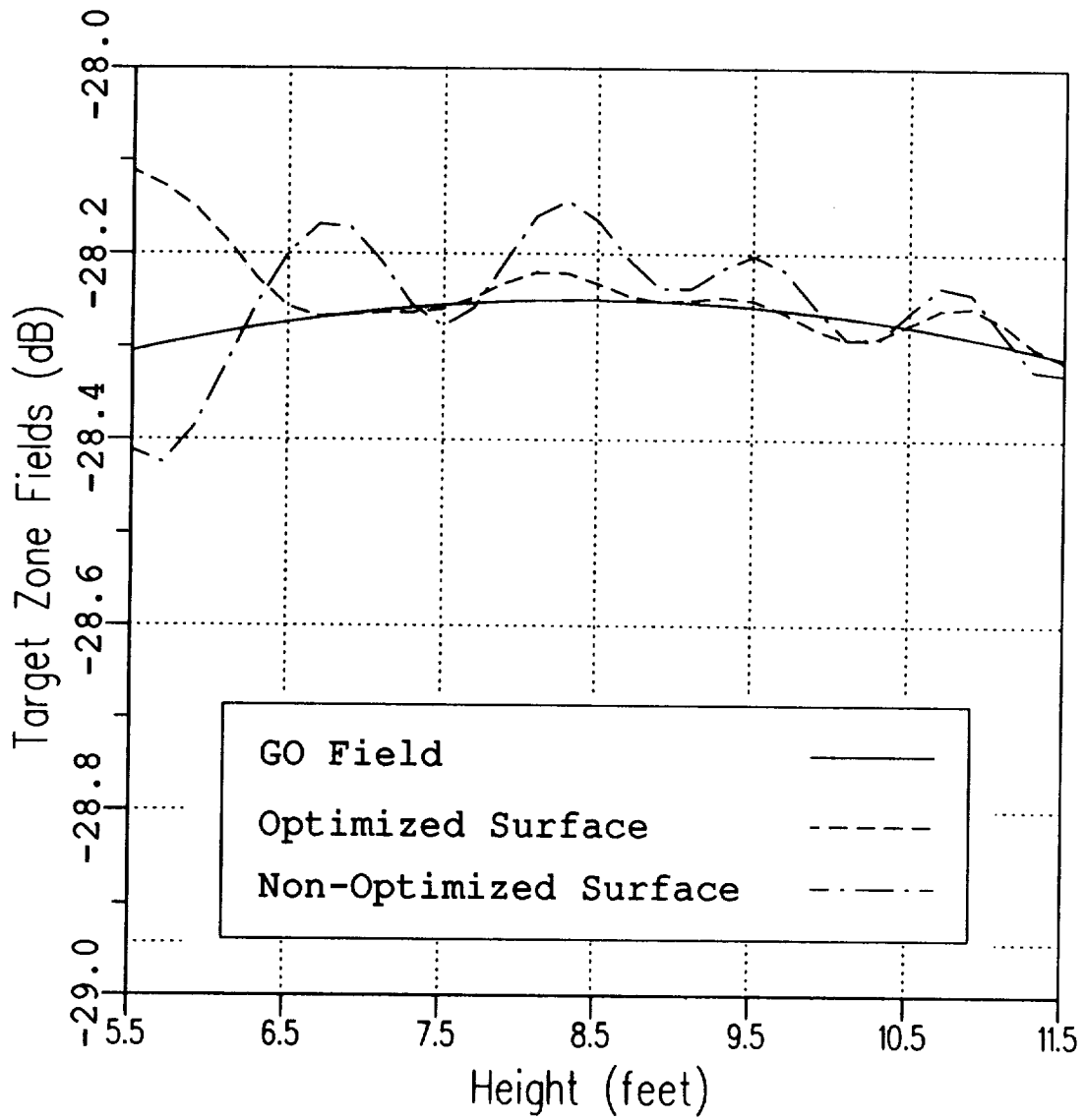
Figure 34: Total scattered fields for a vertical cut through the center of the target zone ($x = 0$).
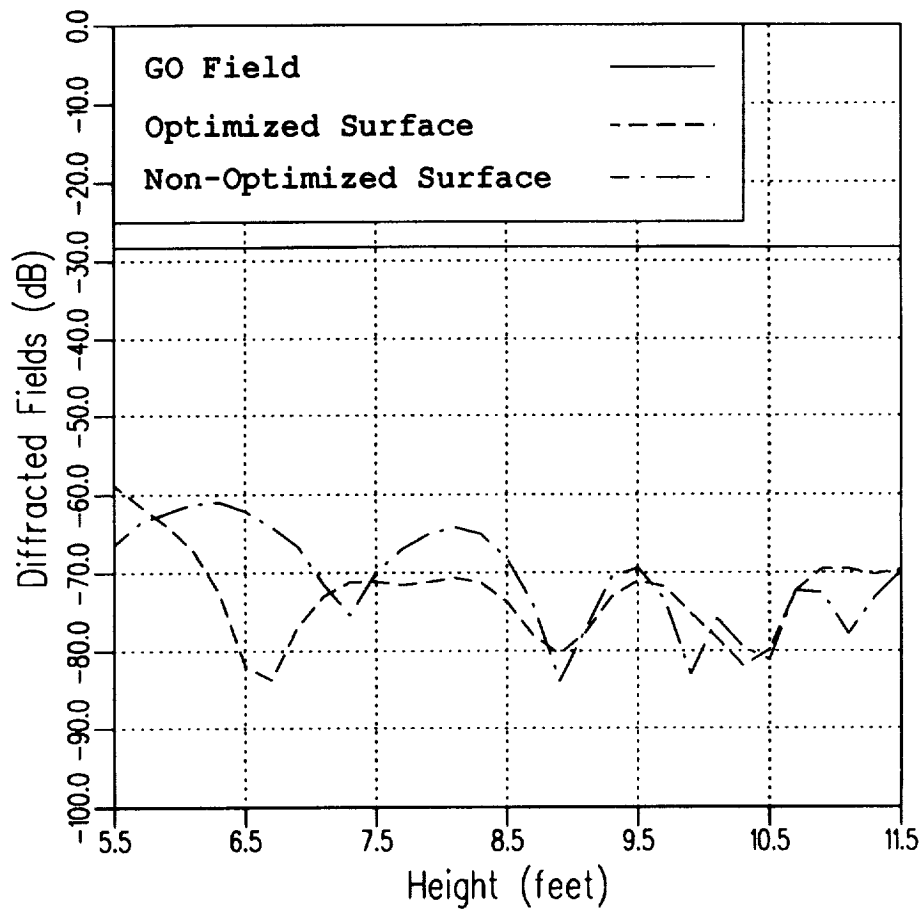
69

Figure 35: Diffracted fields for a vertical cut through the center of the target zone ($x = 0$).
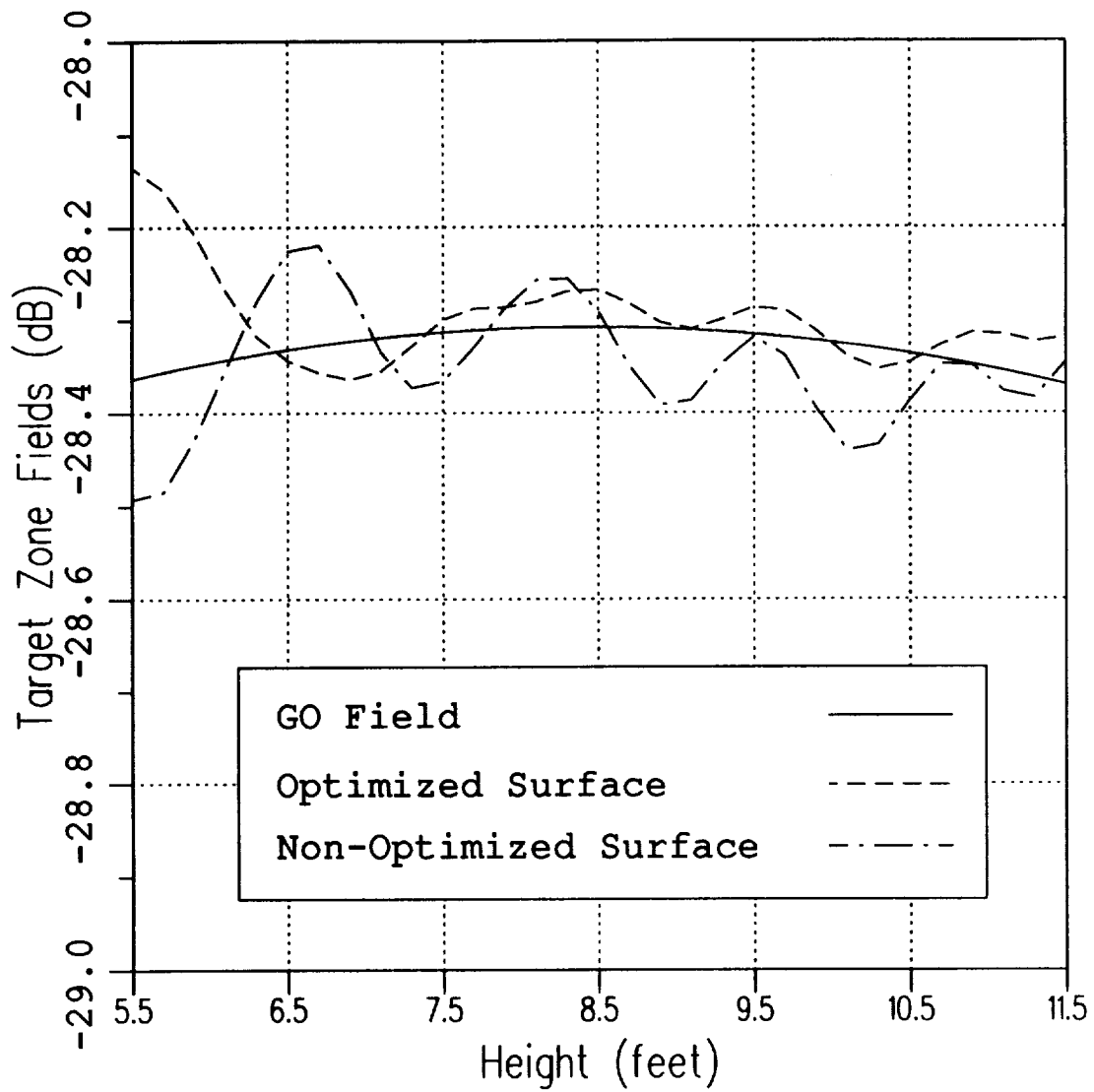
Figure 36: Total scattered fields for a offset vertical cut in the target zone $(x = 3')$.
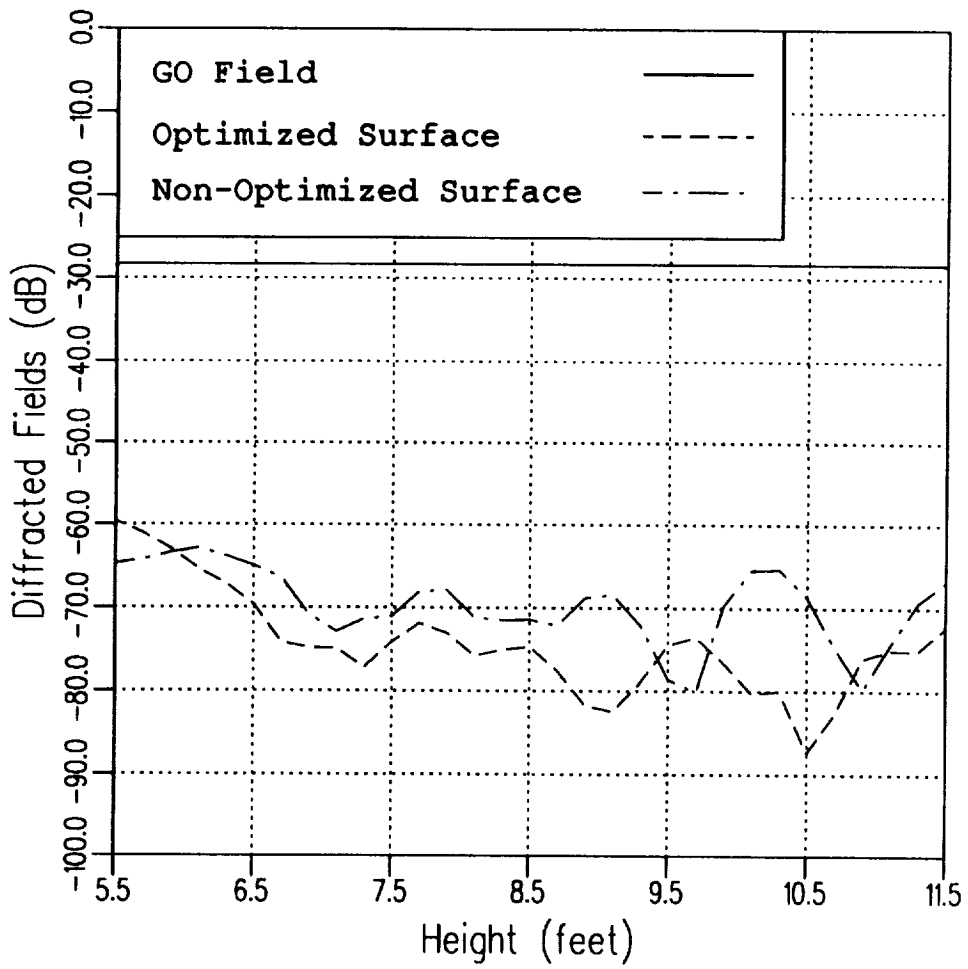
Figure 37: Diffracted fields for a offset vertical cut in the target zone ($x = 3'$).

the fields shown in Figure 36 are the same as the fields along a vertical cut at $x = -3'$. Again, the total scattered fields for both reflectors oscillate around the GO level. The peak to peak variation in the oscillations is slightly lower for the optimized reflector. The diffracted fields for this cut are shown in Figure 37. Note that the diffracted fields for both reflectors are at least 30 dB below the GO fields. Therefore, the performance of the reflectors has not degraded much toward the edge of the target zone.

4.3 Scattered fields along horizontal cuts

Figure 38 shows the scattered fields in the target zone along a horizontal cut when the vertical displacement (y) is 6.5$'$. This cut is also 1$'$ from the junction of the reflector. Also, this cut is the most strongly influenced by the diffracted fields. This is because the transition region of diffracted fields spreads out farther as the distance from the source of diffraction increases [5]. The bottom junction is the farthest junction from the target zone. Thus, this horizontal cut is most affected by diffracted fields since it is in the transition region of the bottom junction. As seen in Figure 38, the total scattered fields for the non-optimized reflector no longer oscillate around the GO level. They have been displaced due to the strong diffracted fields from the lower junction. Note that the total scattered fields for the optimized reflector still oscillate around the GO level in a similar manner to the vertical cuts. The reason the diffracted fields are so strong near the bottom junction for the non-optimized reflector is that the blending parameters for the top junction were used to generate the entire blended rolled edge. This can be seen in Figure 39 where the diffracted fields for the two reflectors are plotted. From this figure, the diffracted fields for the optimized reflector are significantly lower than the diffracted fields for the non-optimized reflector.

Figure 40 shows the scattered fields in the target zone for a horizontal cut with a vertical displacement of 8.5$'$. The total scattered fields for the non-optimized reflector are still slightly displaced above the GO field level. The total scattered fields for the optimized reflector oscillate around the GO level. Figure 41 shows the diffracted fields for this cut. Note that the diffracted fields for both reflectors are at least 35 dB below the GO field.

Figure 42 shows the scattered fields in the target zone for a horizontal cut with a vertical displacement of 10.5$'$. This cut is 1$'$ from the top junction of the paraboloid. For this cut the total scattered fields for both reflectors are almost the same until the horizontal displacement is 2$'$. After this point, the ripple in the oscillations of the scattered fields for the optimized reflector are slightly lower than those of the non-optimized reflector. The diffracted fields for both reflectors are shown in Figure 43. Note that the diffracted fields for both reflectors are at least 35 dB below the GO level.

4.4 Summary

The performance of a parabolic reflector with two different blended rolled edge terminations was presented. The scattered fields from the reflector with a blended rolled edge generated from a fixed set of blending parameters was compared to the scattered fields from a reflector with a blended rolled edge generated from a varying set of optimized blending parameters. Both reflectors showed good performance. Thus, the design procedure presented in this work leads to good blended rolled edges. The optimized reflector showed improved performance in terms of the peak to peak field variation over the whole target zone. This was especially true near the bottom of the target zone. A summary and general conclusion of this work are presented next.
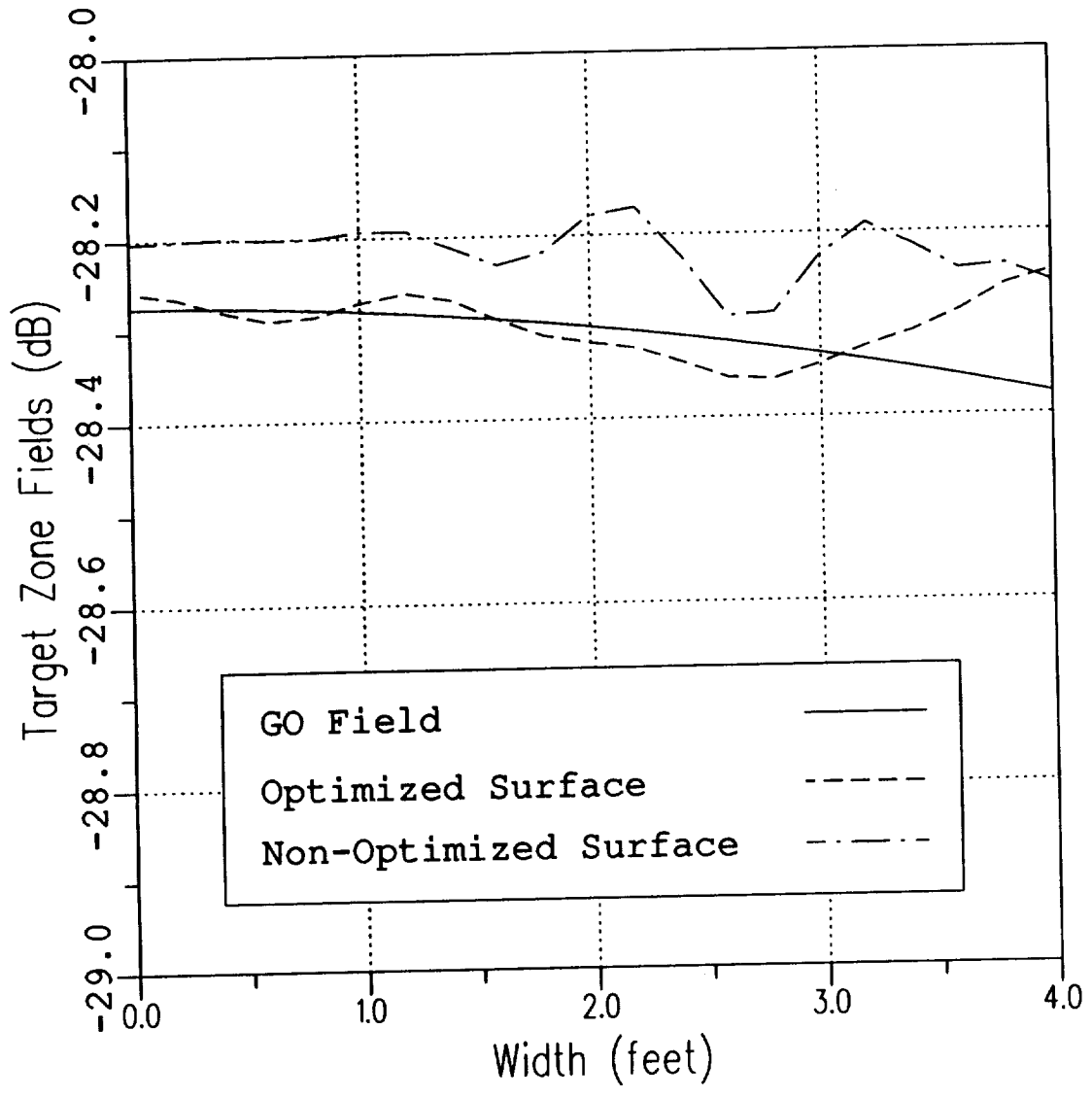
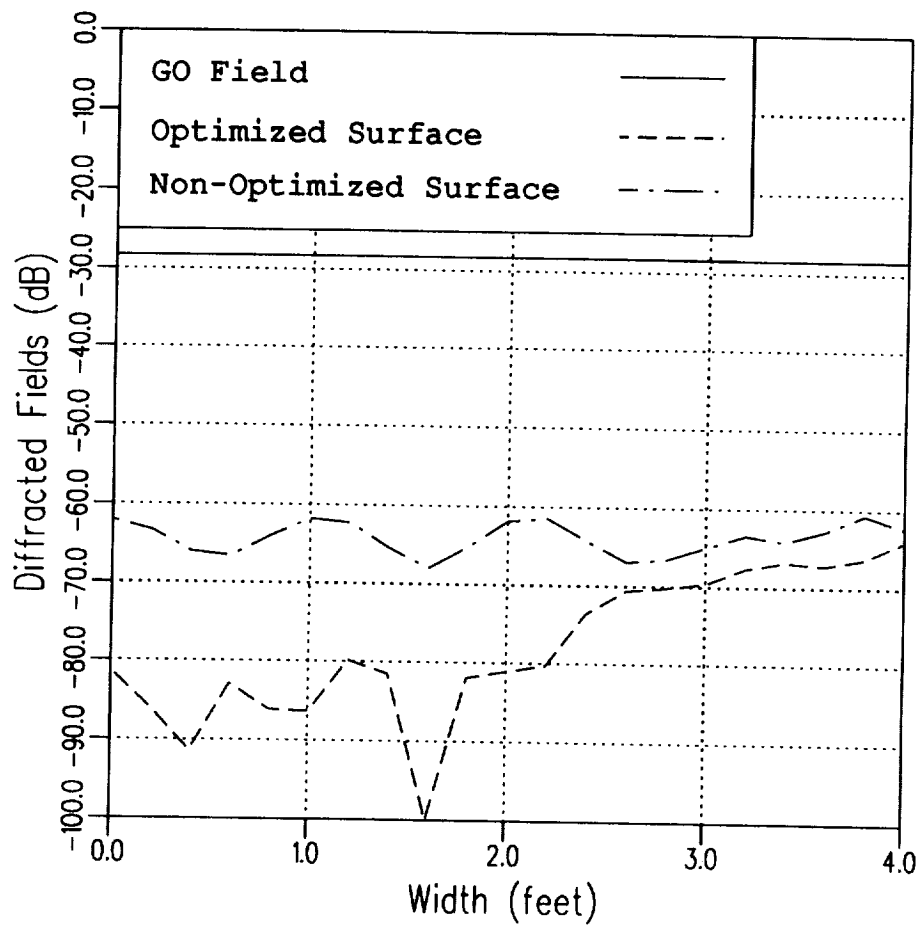Figure 38: Total scattered fields for a offset horizontal cut in the target zone $(y = 6.5')$.

Figure 39: Diffracted fields for a offset horizontal cut in the target zone ($y = 6.5'$).
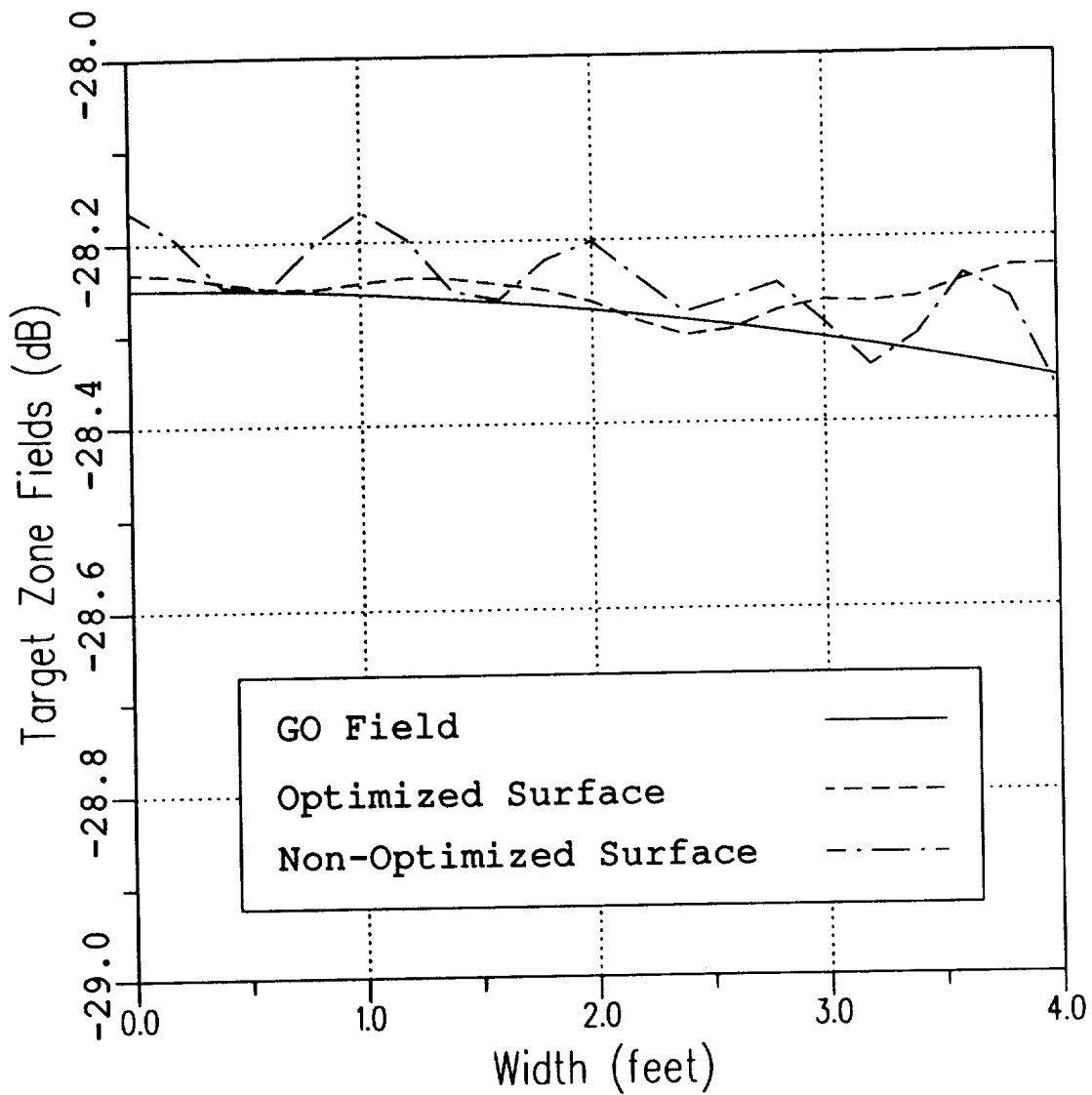
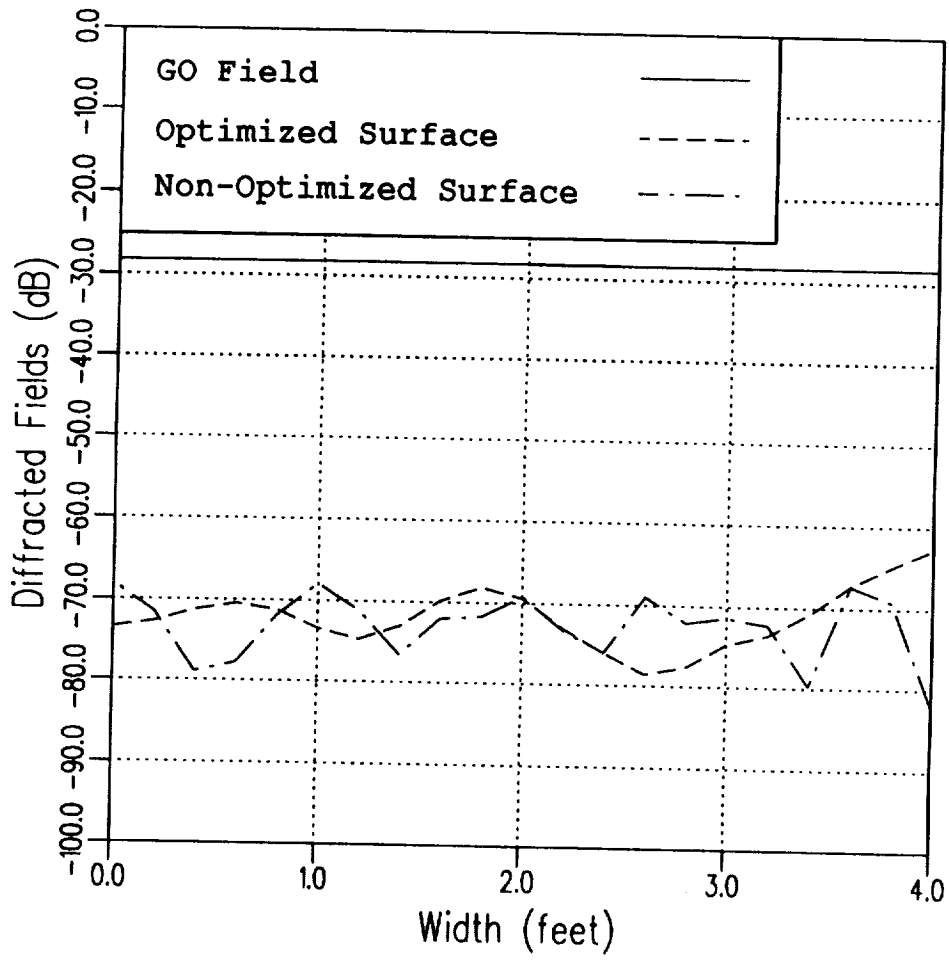Figure 40: Total scattered fields for a offset horizontal cut in the target zone $(y = 8.5')$.

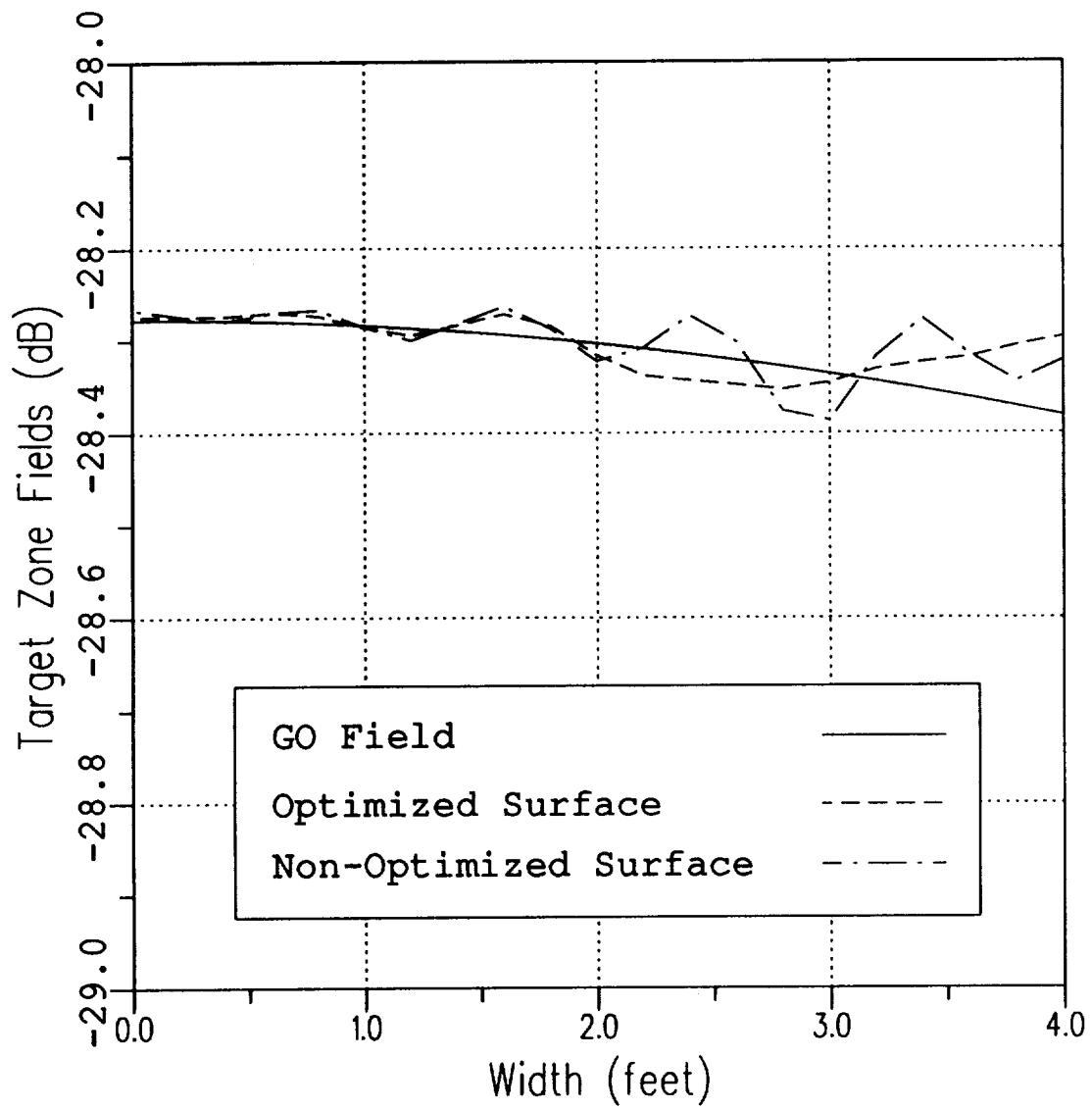Figure 41: Diffracted fields for a offset horizontal cut in the target zone ($y = 8.5'$).

Figure 42: Total scattered fields for a offset horizontal cut in the target zone $(y = 10.5')$.
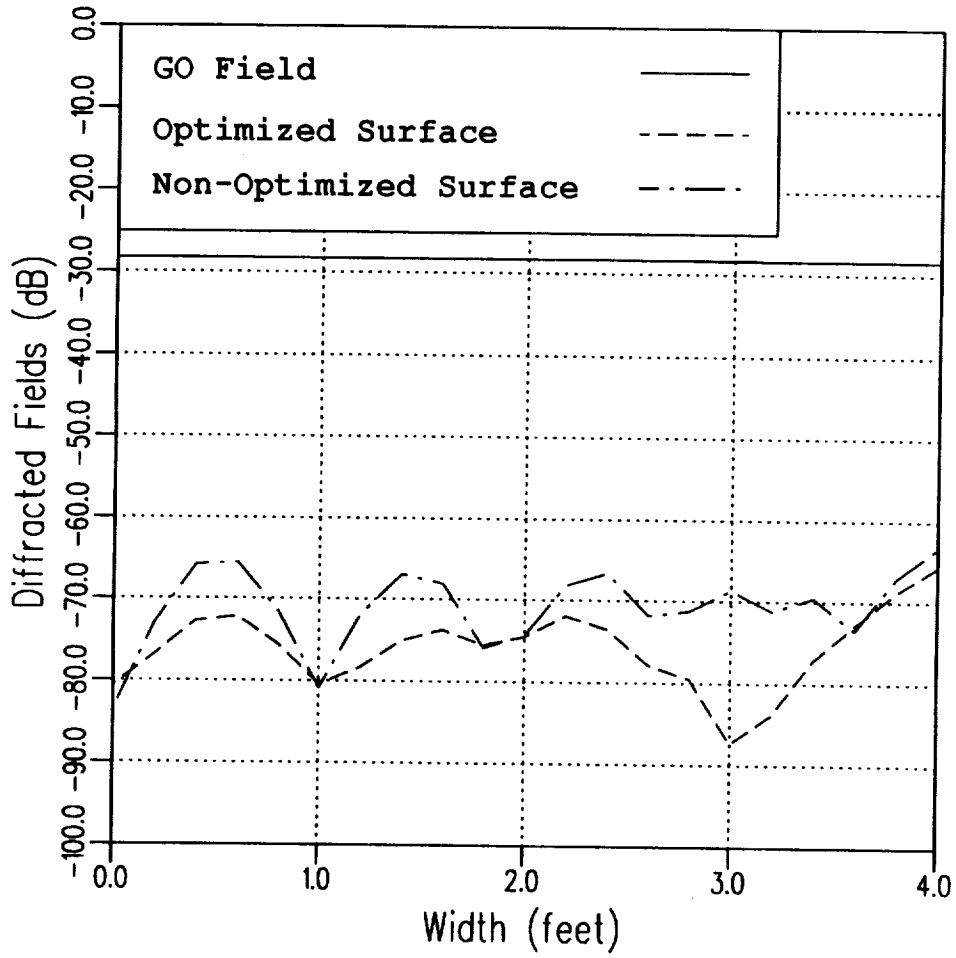
79

Figure 43: Diffracted fields for a offset horizontal cut in the target zone
$(y = 10.5')$.

CHAPTER V

SUMMARY AND CONCLUSIONS

The objective of this research was to develop a procedure to design blended rolled edges for compact range main reflectors. The reflector can have an arbitrarily shaped rim and may be center-fed or offset-fed. A blended rolled edge is added to the reflector to reduce the diffracted fields from the rim of the paraboloid. Thus, the design procedure should lead to a rolled edge that minimizes the diffracted fields and satisfies all design constraints. Such a design procedure was developed. The design procedure leads to a reflector that has a smooth and continuous surface and has a continuous radius of curvature at the junction between the paraboloid and the blended rolled edge. The design procedure guarantees that the reflector will fit in the specified area while minimizing the diffracted fields.

In the design procedure, for each point on the rim of the paraboloid, a rolled edge plane is defined. This rolled edge plane is unique and guarantees a continuous rolled edge. The elliptical section to be blended with the paraboloid at each specific point on the junction contour lies in this rolled edge plane. However, this rolled edge plane may not contain the focal point of the paraboloid. This is especially true for offset reflectors. Thus, the design procedure developed by Gupta *et al.* [7] can not be applied directly. To solve this problem, the concept of an equivalent parabola was introduced. The equivalent parabola has its focus in the rolled edge plane and traces the part of the main reflector paraboloid which lies in the rolled

edge plane. The equivalent parabola was used to design a blended rolled edge for each point on the junction contour. It was shown that the parameters (focal length and junction height) of the equivalent parabola varied along the junction contour. Thus, it was necessary to optimize the blending parameters for each point on the junction contour. However, the variation of the equivalent parabola parameters were very gradual. Thus, the blending parameters need to be optimized only for a limited number of junction contour points. Interpolation was used to find the blending parameters for the intermediate junction contour points.

Since the variation in the blending parameters along the junction contour is so gradual, it is anticipated that a computer code could be developed to optimize the blending parameters for all points on the junction contour starting with a single set of optimized blending parameters. Such a computer code should be developed in the future.

APPENDIX A

DEFINING THE JUNCTION CONTOURS

In this appendix, the defining equations for three different junction contours are presented. The xy-projections of the three contours are shown in Figure 44 [5].

A.1 Concave junction contour

The concave edge contour [5] is formed by considering a rectangle in the xy-plane. This rectangle, referred to as the "defining rectangle", has absolute maximum x dimensions defined as x_{min}, x_{max} and absolute maximum y dimensions defined as y_{min} and y_{max}. These are the same dimensions as the xy-projection of the main reflector including the blended rolled edges and should be equal to the available space for the main reflector. The xy-projection of the target zone is considered to have x-dimensions of x_{left}, x_{rht} and y-dimensions of y_{bot} and y_{top}. The center of the defining rectangle coincides with the center of the xy-projection of the target zone. Radial lines are drawn from the center of the defining rectangle to its border. The concave edge is formed by the locii of the points on the radial lines that are a fixed distance, r_e, from the border of the defining rectangle as shown in Figure 45. The parameter r_e should be set equal to the height of the rolled edge and will determine the amount of concavity of the junction contour. The relations between the defining rectangle and the xy-projection of the target
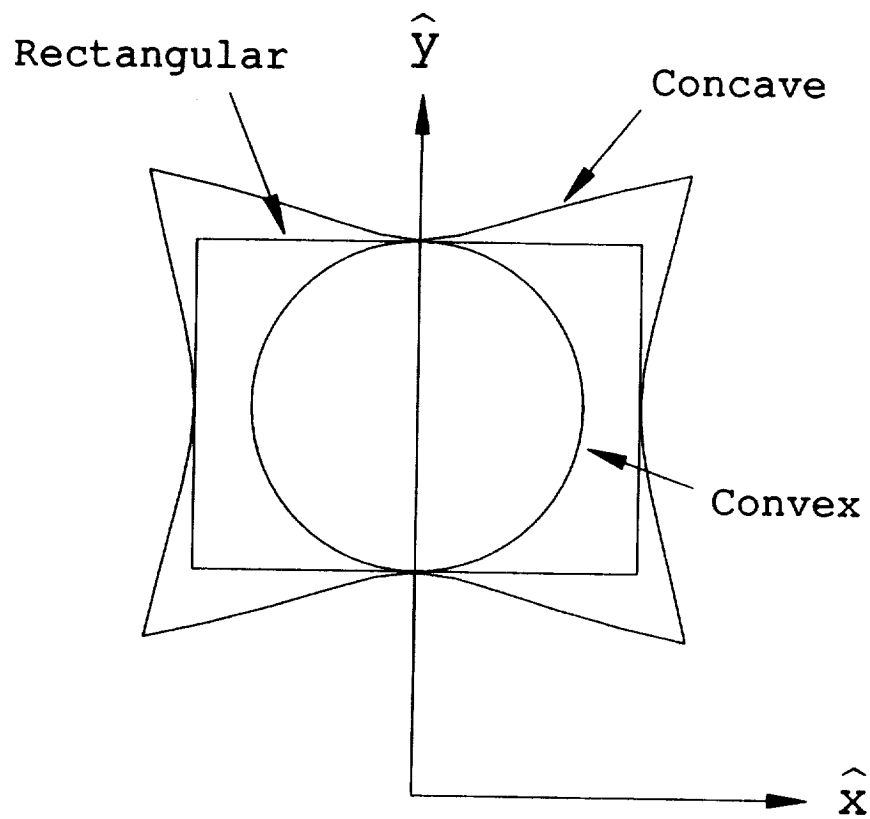
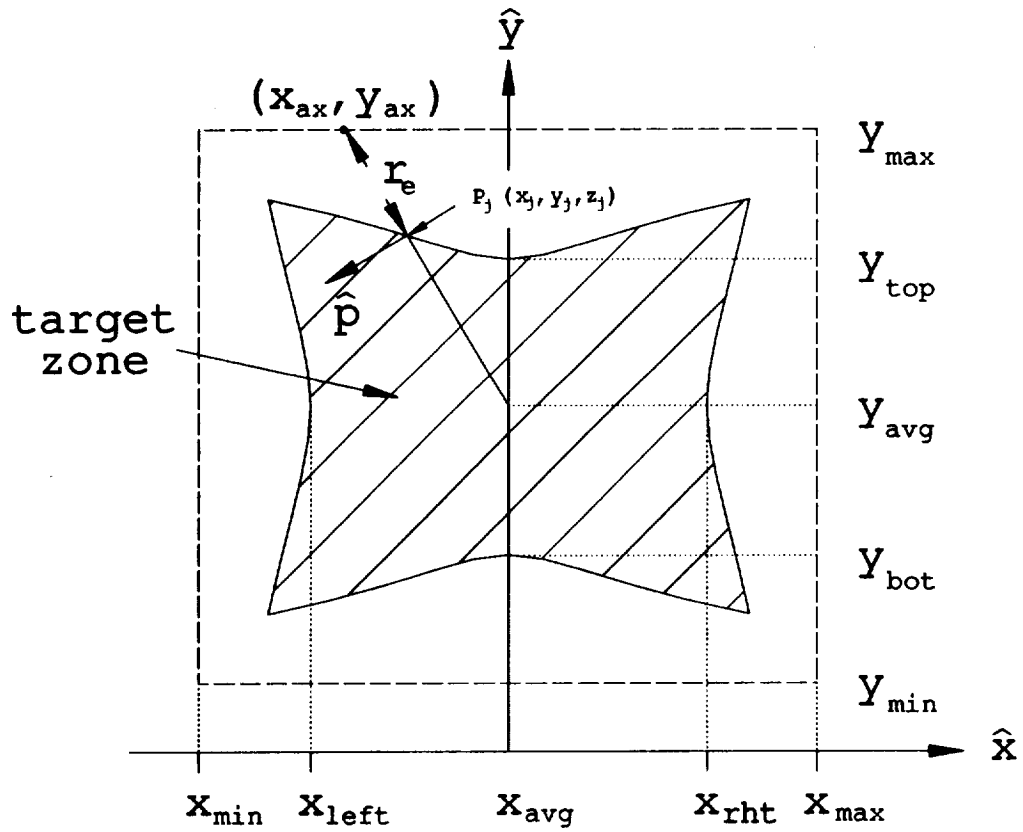Figure 44: xy-projection of the reflector with different edge contour shapes.

Figure 45: Defining rectangle for a concave contour.

zone are given by

$$x_{max} = x_{rht} + r_e \tag{A.1}$$

$$x_{min} = x_{left} - r_e \tag{A.2}$$

$$y_{max} = y_{top} + r_e \text{ , and} \tag{A.3}$$

$$y_{min} = y_{bot} - r_e . \tag{A.4}$$

The center of the xy-projection of the target zone, and thus the center of the defining rectangle, is located at (x_{avg}, y_{avg}), where

$$y_{avg} = \frac{y_{max} + y_{min}}{2} = \frac{y_{top} + y_{bot}}{2} \tag{A.5}$$

$$x_{avg} = \frac{x_{max} + x_{min}}{2} = \frac{x_{rht} + x_{left}}{2} . \tag{A.6}$$

The coordinates of the concave junction can now be found using the defining rectangle. Let (x_{ax}, y_{ax}) be a point on the perimeter of the defining rectangle as shown in Figure 45. The corresponding point on the concave edge contour of the paraboloid is $P_j(x_j, y_j, z_j)$, and is given by

$$x_j = x_{ax} - \frac{r_e(x_{ax} - x_{avg})}{\sqrt{(x_{ax} - x_{avg})^2 + (y_{ax} - y_{avg})^2}} \tag{A.7}$$

$$y_j = y_{ax} - \frac{r_e(y_{ax} - y_{avg})}{\sqrt{(x_{ax} - x_{avg})^2 + (y_{ax} - y_{avg})^2}} \text{ , and} \tag{A.8}$$

$$z_j = \frac{x_j^2 + y_j^2}{4f_c} . \tag{A.9}$$

The entire concave edge contour of the paraboloid can be generated by tracing (x_{ax}, y_{ax}) around the perimeter of the defining rectangle.

A.2 Circular junction contour

The constraint equation for the circular contour is given by

$$y_{max} - y_{min} = x_{max} - x_{min} \ .$$
$$(A.10)$$

The defining rectangle for a circular contour is formed from the maximum dimensions of the reflector. These dimensions are: (x_{max}, x_{min}), and (y_{max}, y_{min}). The relationship between the defining rectangle and the target zone is given by

$$x_{rht} = x_{max} - r_e$$
$$(A.11)$$

$$x_{left} = x_{min} + r_e$$
$$(A.12)$$

$$y_{top} = y_{max} - r_e \ , \text{and}$$
$$(A.13)$$

$$y_{bot} = y_{min} + r_e \ .$$
$$(A.14)$$

Let (x_{ax}, y_{ax}) be a point on the perimeter of the defining rectangle as shown in Figure 46. The corresponding point on the circular junction contour of the paraboloid is $P_j(x_j, y_j, z_j)$, and is given by

$$x_j = (y_{top} - y_{avg}) \left(\frac{x_{ax} - x_{avg}}{\sqrt{(x_{ax} - x_{avg})^2 + (y_{ax} - y_{avg})^2}} \right) + x_{avg} \quad (A.15)$$

$$y_j = (y_{top} - y_{avg}) \left(\frac{y_{ax} - y_{avg}}{\sqrt{(x_{ax} - x_{avg})^2 + (y_{ax} - y_{avg})^2}} \right) + y_{avg} \ , \quad (A.16)$$

and z_j is given by Equation (A.9). The entire circular junction contour can be generated by tracing (x_{ax}, y_{ax}) around the perimeter of the defining rectangle.

A.3 Rectangular junction contour

The absolute maximum dimensions of a reflector with a rectangular junction contour are defined as: (x_{max}, x_{min}), and (y_{max}, y_{min}). The relationship between
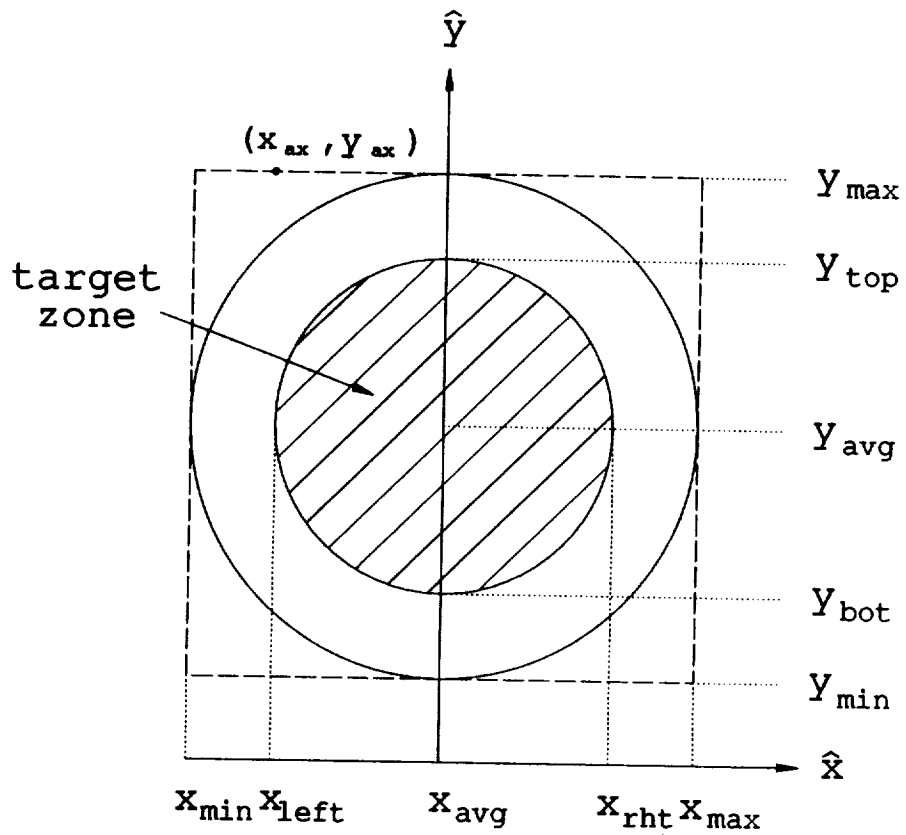
87

Figure 46: xy-projection of a reflector with a circular junction contour.

$C\ 2$

the maximum dimensions and the target zone is given by

$$x_{rht} = x_{max} - r_e \tag{A.17}$$

$$x_{left} = x_{min} + r_e \tag{A.18}$$

$$y_{top} = y_{max} - r_e \text{ , and} \tag{A.19}$$

$$y_{bot} = y_{min} + r_e . \tag{A.20}$$

Let (x_{ax}, y_{ax}) be a point on the perimeter of the rectangle formed by the target zone as shown in Figure 47. The corresponding point on the rectangular junction contour of the paraboloid is $P_j(x_j, y_j, z_j)$, and is given by

$$x_j = x_{ax} \tag{A.21}$$

$$y_j = y_{ax} , \tag{A.22}$$

and z_j is given by Equation (A.9). The entire rectangular junction contour can be generated by tracing (x_{ax}, y_{ax}) around the perimeter of the rectangle formed by the target zone.
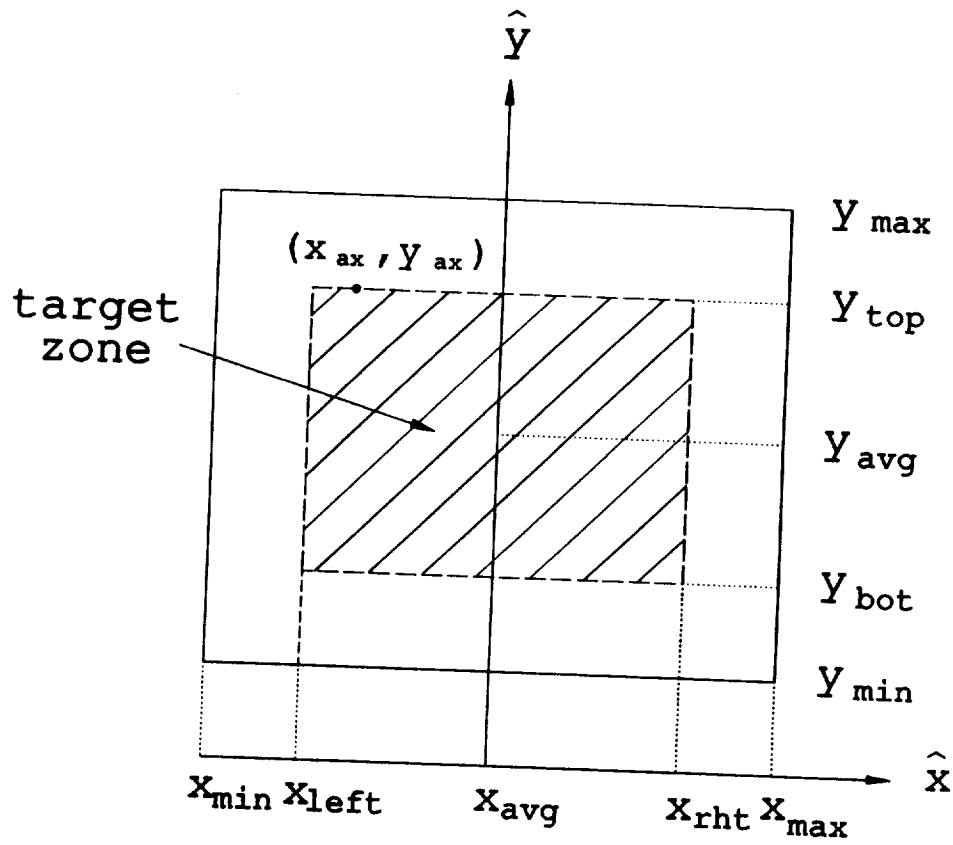
Figure 47: xy-projection of a reflector with a rectangular junction contour.

REFERENCES

[1] R.C. Johnson, H.A. Ecker, and R.A. Moore, "Compact Range Techniques and Measurements", IEEE Trans. Antennas and Prop., Vol AP-17, No 5, May 1969, pp. 568-576.

[2] R.C. Johnson and D.W. Hess, "Performance of a Compact Antenna Range", Dig. IEEE Int. Symp. Antennas Propagat., 1975.

[3] V. Galindo, "Design of Dual-Reflector Antennas with Arbitrary Phase and Amplitude Distributions," IEEE Trans. Antennas and Prop., Vol AP-12, No 7, July 1964, pp. 403-408.

[4] W.D. Burnside, M.C. Gilreath, B.M. Kent, and G.L. Clerici, "Curved Edge Modification of Compact Range Reflector", IEEE Trans. Antennas and Prop., Vol AP-35, No 2, February 1987, pp. 176-182.

[5] C.W.I. Pistorius, *New Main Reflector, Subreflector and Dual Chamber Concepts for Compact Range Applications*, Ph.D. dissertation, Ohio State University, Columbus, 1986.

[6] W.D. Burnside, A.K. Dominek, and R. Barger, "Blended Surface Concept for a Compact Range Reflector", *Proceedings of AMTA '85 Symposium*, Melbourne, FL.

[7] I.J. Gupta and W.D. Burnside, "Design of Blended Rolled Edge for Compact Range Reflectors", *Proceedings of AMTA '87 Symposium*, pp. 259-264, Seattle, Washington.

[8] M.D. Rader and W.D. Burnside, *A Cassegrain Reflector System for Compact Range Applications*, Tech. Report 716148-14, The Ohio State University ElectroScience Laboratory, July 1986.

[9] W.A. Wong, "On the Equivalent Parabola Technique to Predict the Performance Characteristics of a Cassegrain System with an Offset Feed", IEEE Trans. Antennas and Prop., Vol AP-21, No 3, May 1973, pp. 335-339.

[10] T-S Chu and R.H. Turrin, "Depolarization Properties of Offset Reflector Antennas", IEEE Trans. Antennas and Prop., Vol AP-21, No 3, May 1973, pp. 339-345.

[11] I.J. Gupta and W.D. Burnside, "A Physical Optics Correction for Backscattering from Curved Surfaces", IEEE Trans. Antennas and Prop., Vol AP-35, No 5, May 1987, pp. 553-561.

[12] W.D. Burnside and L. Peters, Jr., "Target Illumination Requirements for Low RCS Target Measurements", *Proceedings of AMTA '85 Symposium*, Melbourne, FL.

[13] D.R. Rhodes, "On Minimum Range Radiation Patterns", Proc. IRE, Vol 42, September 1954, pp. 1408-1410.

[14] M. Athans, M.L. Dertouzous, R.N. Spann, and S.J. Mason, *Systems, Networks, and Computation Multivariable Methods*, McGraw-Hill, 1974.

[15] I.J. Gupta, Personal communication, The Ohio State University Electro-Science Laboratory.

[16] D.J. Struik, *Differential Geometry*, 2nd. Ed., Addison-Wesley, 1961.

[17] L.W. Johnson and R.D. Riess, *Numerical Analysis*, Addison-Wesley, 1982, pp. 194-199.